A SNAPSHOT OF AN EARLY PERMIAN ECOSYSTEM PRESERVED BY EXPLOSIVE VOLCANISM: NEW RESULTS FROM THE CHEMNITZ PETRIFIED FOREST, GERMANY

Author(s): RONNY RÖßLER , THORID ZIEROLD , ZHUO FENG , RALPH KRETZSCHMAR , MATHIAS MERBITZ , VOLKER ANNACKER , and JÖRG W. SCHNEIDER

Source: PALAIOS, 27(11):814-834. 2012.
Published By: Society for Sedimentary Geology
URL: http://www.bioone.org/doi/full/10.2110/palo.2011.p11-112r

PALAIOS
Emphasizing the impact of life on Earth's history

PALAIOS, 2012, v. 27, p. 814–834
Research Article
DOI: 10.2110/palo.2011.p11-112r

1926 SEPM Society for Sedimentary Geology

A SNAPSHOT OF AN EARLY PERMIAN ECOSYSTEM PRESERVED BY EXPLOSIVE VOLCANISM: NEW RESULTS FROM THE CHEMNITZ PETRIFIED FOREST, GERMANY

RONNY RÖßLER,[1]* THORID ZIEROLD,[1] ZHUO FENG,[1,2] RALPH KRETZSCHMAR,[1] MATHIAS MERBITZ,[1] VOLKER ANNACKER,[1] and JÖRG W. SCHNEIDER[3]

[1]*DAStietz, Museum für Naturkunde, Moritzstraße 20, D-09111 Chemnitz, Germany, roessler@naturkunde-chemnitz.de, zierold@naturkunde-chemnitz.de, r.kretzschmar@kieseltorf.de, prc-team-chemnitz@gmx.de, volker@psaronius.de;* [2]*Yunnan Key Laboratory for Palaeobiology, Yunnan University, Kunming 650091, People's Republic of China, jumperfeng@126.com;* [3]*Geological Institute, Technische Universität Bergakademie Freiberg, Bernhard-von-Cotta-Strasse 2, 09596 Freiberg, Germany, schneidj@geo.tu-freiberg.de*

ABSTRACT

A recently excavated locality in the Chemnitz Petrified Forest, lower Permian in age and occurring within the Leukersdorf Formation of the Chemnitz Basin, Germany, provides evidence for an outstanding fossil assemblage buried *in situ* by pyroclastics. The environment is interpreted as forested lowland that sheltered a dense hygrophilous vegetation of ferns, sphenophytes, and gymnosperms, as well as a diverse fauna of reptiles, amphibians, arthropods, and gastropods. A detailed measured section of the outcrop documents the early volcanic history of the Chemnitz fossil forest, including a paleosol that shows the root systems of *Psaronius* tree ferns, *Arthropitys* calamitaleans, and *Medullosa* and *Cordaixylon* gymnosperms in the same horizon. Fifty-three trunks are still standing upright and rooted at their place of growth, providing evidence that the top of the paleosol was the land surface on which the forest grew, thereby offering insights into the original plant community structure and density. Taphonomic analysis of both the petrified and adpression-fossil assemblages enable us to reconstruct the direction, estimate the violence and extent of the volcanic events, and their effects on the entire ecosystem. A complete dataset of three-dimensional coordinates resulting from three and one-half years of continuing excavation and study permits the recognition of organ connections and results in the first reconstructions of the excavation site, the floral elements, and the plant community as a whole.

INTRODUCTION

In fossil forests ancient trees from the geological past have been fossilized in growth position. One of these fossil forests is known from Chemnitz, Germany, where an early Permian landscape was buried instantaneously by volcanic ash, preserving autochthonous and parautochthonous fossil assemblages (Sterzel, 1875; Barthel, 1976; Rößler, 2001). What makes this fossil Lagerstätte so special in comparison with other fossil forests with tree stumps preserved *in situ* is the historical importance of the Chemnitz fossil forest. Collecting at this site dates back to the early 18th century, and many collections worldwide house exhibition-quality specimens from the Chemnitz Petrified Forest. Specimens from this site provided the basis for introduction of fossil plant names reaching back to the early days of paleobotany. Several genera of common late Paleozoic plants were first described from Chemnitz, the type locality of *Psaronius, Tubicaulis, Calamitea*, and *Medullosa* (Cotta, 1832).

The majority of finds were made in the late 19th and early 20th centuries. Since the 1990s many new specimens have been recovered during construction work, but all of them were unintentional, because most of the fossil forest has been developed into an urban area. Hence, the possibility of reconstructing both whole plants and the paleoenvironment in which they grew was limited. Nevertheless, based on accidental finds and on specimens from historical collections, the Chemnitz fossil Lagerstätte has been reinvestigated in the last decade. Research on specific taxa, particularly on calamitaleans and ferns, has resulted in new observations and taxonomic revisions (Rößler, 2000; Rößler and Noll, 2006, 2007, 2010).

With this in mind, the Museum für Naturkunde Chemnitz carried out a systematic and well-documented scientific excavation of the Chemnitz Petrified Forest for three and one-half years (2008–2011). The excavation site is one of the very few remaining areas that have not been disturbed by building activities and, thus, offered a unique chance to study the fossil forest *in situ*. Specific objectives of the excavation were to find evidence for connections of organs in the Chemnitz plants, and to record coordinates in three-dimensional (3D) space for each find, enabling 3D reconstructions of the excavation site, the unearthed plant fossils, and the plant community. In addition, we aimed to investigate the volcanic and sedimentary rocks in the outcrop area to acquire a clearer understanding of the volcanic events and how they affected the ecosystem.

Our preliminary data consist of a large number of exceptional finds, 3D coordinates, and detailed field observations (Kretzschmar et al., 2008; Rößler et al., 2009, 2010). Unique features that have been documented here for the first time are: (1) the presence of rooting structures of several taxa that are preserved *in situ* in a single horizon, (2) the occurrence of foliage and reproductive organs associated with petrified stems and branches, and (3) the presence of various animal remains found together with the plants, including reptiles still showing the original body outlines.

The way in which pyroclastics preserve a standing vegetation within its ecological context was recently described by Opluštil et al. (2004, 2009) and Libertín et al. (2009) in their comprehensive studies from the Pennsylvanian (Bolsovian) of Central Bohemia. Preservation by tuffaceous deposits, however, is not restricted to a particular basin or stratigraphic level. Comparable occurrences have been reported from the Pennsylvanian–Permian boundary in the Puertollano Basin in Central Spain (Wagner, 1989) and the Döhlen Basin in southeast Germany (Rößler and Barthel, 1998), as well as from the Permian of China (Hilton et al., 2001, 2004; Pfefferkorn and Wang, 2009).

Thus, the new finds from Chemnitz allow complex inferences on the ecology and environment of this Permian petrified forest, being more detailed than has been possible before. The outstanding role of so-called T^0 assemblages, fossil forests that are buried in growth position within a geological instant, as recently discussed by DiMichele and Falcon-Lang (2011), will be emphasized. We will set up and complete a database to document the fossil record of our study site to develop a model of the ecosystem. With the help of this data source, the use of 3D visualization, and the resulting model, we aim to apply improved and more sophisticated techniques in paleobotany, offering new perspectives for the reconstruction of plant organs, individual plants at their

* Corresponding author.
Published Online: December 2012

 0883-1351/12/0027-0814/$3.00

site of growth, paleoenvironments, and ultimately processes that lead to their preservation.

MATERIALS AND METHODS

The Museum für Naturkunde Chemnitz carried out the first scientific excavation of the fossil forest within the city limits of Chemnitz (50°51′58.68″N, 12°57′32.54″E) from April 2008 to October 2011 (Fig. 1). The site is located in the middle of a residential area, but fortunately older anthropogenic influences could be excluded in the excavation area, because the excavation site is one of the very few lots that were never built upon. The dimensions of the excavated area were 24 m by 18 m, and a depth of at least 5 m, which left ~130 m^2 at the bottom of the pit. Sediment at the top (Units S1 and S2) that was obviously reworked and belongs to the Quaternary cover was taken away mechanically without any further documentation. The underlying rock was then gradually removed by hand. Digging downward was undertaken stepwise in 30-cm-thick layers, or according to distinct units. Specimens were categorized in associated, numbered parts. For example, code KH was used for petrified remains, while attached branches were given separate KH numbers. Since organic matter is rarely preserved or largely absent in these fossil trees, we adopt the terminology given in Taylor et al. (2009) and characterize this material as petrifactions. Protocols (code FP) consist of a sketch with the orientation and position of the fossils, general information such as the date of excavation, the processor and associated documents (photographs, storage), and data control fields. The main part of the document contains information on the fossils: part numbers, measurements, and brief descriptions. Such 3D records were made for every petrified specimen in each unit.

A huge number of data and specimens were recovered. In all, about 860 collection boxes were filled with 630 petrified trunks and isolated branches of various plant groups. In total, 53 trunks still standing upright in growth position were found. In addition, about 1,200 adpressions (code TA) of associated megafloral and megafaunal fossils and 635 rock samples (code GP) for future sedimentological, geochemical, and volcanological studies were collected, recorded, and measured in three dimensions. Apart from petrifications, various types of foliage are found in Chemnitz. These are adpressions in which the organic matter is replaced by mineral matter. In many cases the original plant material is only partially compressed, and hence exhibits a 3D aspect of the fossils. Since the term compression is defined for plants compressed by sediment, in which the plant tissue is still preserved as a highly coalified layer (Shute and Cleal, 1987; Bateman, 1991), this term cannot be used because coaly matter is lacking. For the same reason the term adpression that has been defined as a mixture of compression and impression states is inappropriate. As no adequate term appears to be available for this quite common type of preservation, we provisionally use the term adpression for this mode of fossilization. These adpressions consist of single leaves or pinnules, reproductive structures, roots, and nearly complete fronds. For the first time, several vertebrates and invertebrates were recovered from the Chemnitz fossil Lagerstätte. Among them five reptile skeletons, several amphibians, diplopods, remains of the giant arthropod *Arthropleura*, arachnids (trigonotarbids, several scorpions, and a whip scorpion), more than one hundred gastropod remains, and disarticulated bones were documented. A considerable portion of the material still remains to be identified, however.

A standard collecting procedure was developed to reveal the spatial relationships between the fossils in this T^0 deposit and to obtain the maximum possible information. We used a 3D grid to document the position and orientation of all fossils and geological structures. A flexible grid structure was installed on the solid rock surface with the permanent point of reference in the upper southern corner of the pit. All measurements were made relative to a global coordinate system.

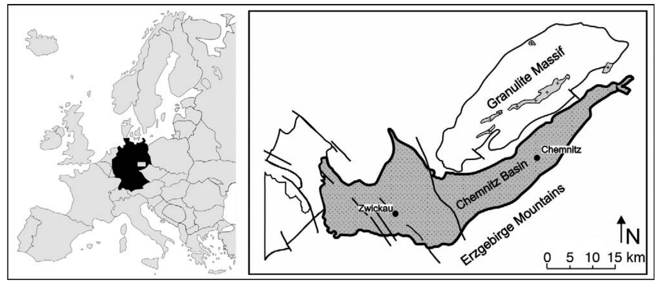

FIGURE 1—Location map of the study area.

For easy differentiation, the y-axis was subdivided into letters and the x-axis into numbers, every meter. Values on the z-axis are positive downward, relative to the permanent reference point. Using fixed reference points, temporary, locally applied grids were used for manual measurements, particularly during the 2008 excavation. The accuracy of this coordinate system was tested from time to time. In 2009, the use of a tachymeter was introduced, 3D coordinates were recorded in files, and allocation took place by means of numbered reference points. More than 10,000 reference points for specimens, surfaces, and bleached zones were recorded during the excavation.

Rock samples were collected systematically. In Unit 3, oriented specimens were sampled every 2 m horizontally and every 1 m vertically. Additional samples for geochemical analyses were taken at a distance of every 4 m horizontally and every 1 m vertically. In the lower part of the excavation pit (Units S4 to S6), oriented specimens from the entire section were collected every 2 m horizontally. Additional sampling was carried out to save striking sedimentological features or for specific research purposes.

The position and orientation of fossils and structures were recorded by extensive photograph documentation; about 9,000 photographs, totaling 600 FO numbers, were taken. Photographs were labeled with a photo number (FO), location, specimen or structure number, date, scale, and orientation (x- and y-axes). Another 9,000 photos document the excavation process in addition to more than 600,000 webcam images and 6 hours of digital video.

Unit S3 shows many large, light-green- to gray-colored haloes surrounding the fossil trunks and branches. Outlines of these bleached haloes were measured every 30 cm, both horizontally and vertically. The resulting data provide a basis for the visualization of the bleached zones as cloudlike objects in a 3D model that is closely related to the silicified plants (see Fig. 10C). In Unit S6, in which plant remains such as roots are more abundant, the bleached zones were simply recorded by protocols or photographs. About 70 bleached zones (BZ) were recorded separately.

Unit S4, a thin, strongly lithified layer, is characterized by the common presence of cracks. For this layer, a 2D record was created (code S4P), which was combined with a 3D measurement of the upper surface. Crack-surrounded slabs were consecutively numbered (code SL), sketched, and marked with reference points at distances dependent on topographic changes and determined by local slab thickness. While excavating Unit S4, slab thickness was measured by hand, and the occurrence of adpressions was noted in a sketch. 110 slabs were recorded in 77 protocols, covering an area of approximately 130 m^2.

Unit S5 is multilayered, and contains abundant adpressions at its base. The protocol type (code S5P) was specially created for the so-called leaf horizon records to include data on the 2D location and orientation as well as descriptions, and supplementary information on specimens within an area of 2 m^2, documented using a locally applied grid. The upper surface of Unit S5 was measured in three dimensions, and the distances between points depended on topographic changes. The upper 20 cm of Unit S6 were documented in the same way, with 3D measurements of the surface and afterward the 2D recording of specimens (code S6P). Two additional, small (~1–2 m^2) sections for further analysis in the lab were collected reaching a depth of 1.2 m and 2 m, respectively, beneath the top of Unit S6.

Nearly all fossil remains in Units S3 and S4 were collected. In Units S5 and S6, however, only the most instructive finds were collected; small fragments were identified on the spot and marked in the protocol, since the majority was incomplete or badly preserved.

Nearly all silicified specimens, bleached haloes, and unit surfaces were integrated into a preliminary, 3D virtual model using Blender 3D computer graphics software (Fig. 10C).

LOCALITY, AGE, AND BIOSTRATIGRAPHY

The origin of the Chemnitz Petrified Forest is closely related to the explosive rhyolithic volcanism that occurred on a widespread scale during the early Permian (Schneider et al., 1995; Roscher and Schneider, 2006). One of the eruptions in the area of present-day Chemnitz resulted in the formation of a pyroclastic sequence referred to as the Zeisigwald Tuff Horizon in the upper Leukersdorf Formation (Fischer, 1990; Schneider et al., 2011). Amphibian remains of the *Melanerpeton pusillum-Melanerpeton gracile*–Zone indicate a position in the European highest Lower Rotliegend (Werneburg and Schneider, 2006; Schneider and Werneburg, 2011). The absolute age of this volcanic event of about 290.6 ± 1.8 Ma was recently determined by SHRIMP U–Pb measurements on zircons (K.-P. Stanek, personal communication, 2009), which corresponds to the late Asselian–early Sakmarian. This has also been supported by a rich palynoflora dominated by the saccate pollen taxa *Potonieisporites* spp., *Florinites ovalis,* and *Vesicaspora* spp., and by *Vittatina* sp. from the palustrine Rottluff Coal in the lower part of the Leukersdorf Formation (Döring et al., 1999). This association shows great similarities of this stratigraphic level and the late Asselian Slavjanskaja Svita of the Donetsk Basin reference section.

The Leukersdorf Formation (Fig. 2) consists of approximately 800 m of sedimentary and volcanic deposits, dominated by red beds that were formed in a semiarid regional climate (Schneider et al., 2011). The alluvial plain sediments belong to the wet red beds type according to Schneider et al. (2010) and were deposited during the late early Cisuralian wet phase D (Roscher and Schneider, 2006). Apart from common tiny rootlets, this formation basinwide rarely shows any evidence of plant growth. In this respect, the Chemnitz fossil Lagerstätte is an unusual, very local assemblage with a rich forest flora that is characterized by a dominance of hygrophilous plants and a few mesophilous elements.

During the early Permian, increasing floristic differentiation took place that resulted in distinct plant communities (Kerp, 1996; Barthel, 2001; DiMichele et al., 2011). Depending on local hydrologic conditions, small, damp areas to larger, extended drylands may have developed (DiMichele et al., 2006), and any such deposits still preserved in the geologic record may comprise many hiatuses. Nevertheless, at the fossil forest level in Chemnitz we recognize a plant assemblage typical of the Rotliegend that contains pteridosperms such as *Alethopteris schneideri* and *Taeniopteris abnormis*, but also the calamite leaf type *Annularia spicata*.

GEOLOGICAL SETTING: NEW RESULTS

Sedimentary and Volcanic Deposits, and Taphonomic Insights

The excavated section comprises of the lower part of the Zeisigwald Tuff Horizon and its sedimentary basement (Fig. 3). It has been divided into six units (S1–S6). Unit S5 is further subdivided into four distinct lithofacies. Table 1 lists the main characteristics of these units or lithofacies which are described and interpreted below. The rock units below are described in order of their formation, i.e., from the bottom to the top. This description excludes Units S1 and S2 that represent the recent soil horizon overlying weathered runoff hill scree with scattered log fragments and extending down to approximately 1.3 m depth.

Unit S6, Variegated Siltstone.—The 1.85-m-thick Unit S6 consists of a varicolored fine-sandy siltstone with limited amounts of mudstone and fine sandstone. In some places, matrix-supported quartz pebbles of cm size occur. The lower boundary to reddish-brown well-bedded siltstones is confluent. Unit S6 appears to be mainly structureless due to considerable rhizoturbation (Fig. 4A). However, there are parts near the top of Unit S6 that show laterally restricted areas of former horizontal bedding planes. These bedding planes are not only characterized by fine-grained white mica, but also by frequent root mats or plant fragments. The sediment shows a light-green- to gray- or purple-colored mottling. Greenish leached parts are stronger calcite cemented. A level with greenish-gray, calcitic, mm-sized glaebules to dm-large, internally micritic nodules with sparitic rootlet traces (rhizoliths) are intercalated 0.8 to 1 m below the top of Unit S6. Top and base are gradational; nodules occasionally contain chert lenses of authigenic silica.

The surface of Unit S6 exhibits an undulating appearance that generally can be traced vertically as far up as Unit S4. The uppermost pale–reddish brown 5 to 17 cm of Unit S6 are strongly lithified and can be correlated to other outcrops several hundred meters away (Eulenberger et al., 2010). Large sediment slabs show a light–gray-green–colored carbonate-cemented interior, free of dark manganese mud, whereas the majority of former roots are preserved as slightly flattened molds, often filled with dark-brown to black mud. Downward-tapering and branching cavities were also recognized as rhizoliths. Close to the margin of petrified *in situ* trunks, the lithification of the uppermost layer extends deeper. Unit S6 shows *in situ* root systems of several trunks representing different taxa. The roots nearest to the trunk are found as petrifactions, but often preservation decreases in quality further away from the trunk so that only molds, casts, or simply haloes remain. *In situ* rooted bases of wide trunks seem to be better preserved than the smaller ones. Deeper in the section, compaction of all organic inclusions becomes more abundant, while bedding structures become increasingly rare. Compaction-induced deformation is clearly recognizable from folded roots (Fig. 4B).

Besides the commonly observed roots exhibiting various orders of branching or differential preservation, plant litter rarely occurs as impressions. The supposed ground cover and leaf litter, however, seem to be obscured due to the major sliding surface between Units S6 and S5. The few plant remains that could be identified were leafy conifer shoots of varying sizes, cordaitalean and pteridosperm leaf fragments, both cordaitalean and pteridosperm seeds, and small calamitalean leafy shoots (Figs. 4C–D). Large, horizontal pieces of trunks may represent deadwood; the anatomical preservation of these trunks improves the deeper they extend into the sediment (Fig. 4D), although they are significantly weathered or eroded at the S6–S5 boundary. Disarticulated vertebrate bones (Fig. 4G) and casts as well as silicified shell pseudomorphs of terrestrial gastropods, associated with root traces and deadwood, are further elements of the fossil assemblage of this unit (Figs. 4F, H). The gastropods belong to the genus *Dendropupa* and resemble *D. walchiarum* Fischer from the Autunian of France and *D. zarecznyi* Panow from the Lower Permian of Poland (B. Hausdorf, personal communication, 2011). Very recently, several fossil scorpions were found in what was likely the life position in their natural habitat, a few centimeters beneath the soil surface (see Fig. 12C).

Unit S6, Interpretation.—Unit S6 is interpreted as an alluvial paleosol, as indicated by a set of diagnostic criteria for soil formation (cf. Retallack, 2001). The most conspicuous feature is the common presence of roots in different forms of preservation, intensive color mottling, and the occurrence of carbonate glaebules of different sizes. The rooting of plants and other processes involved in soil formation (swelling, shrinkage, pedoturbation, various animal activity) have altered or completely destroyed most preexisting sedimentary structures. The

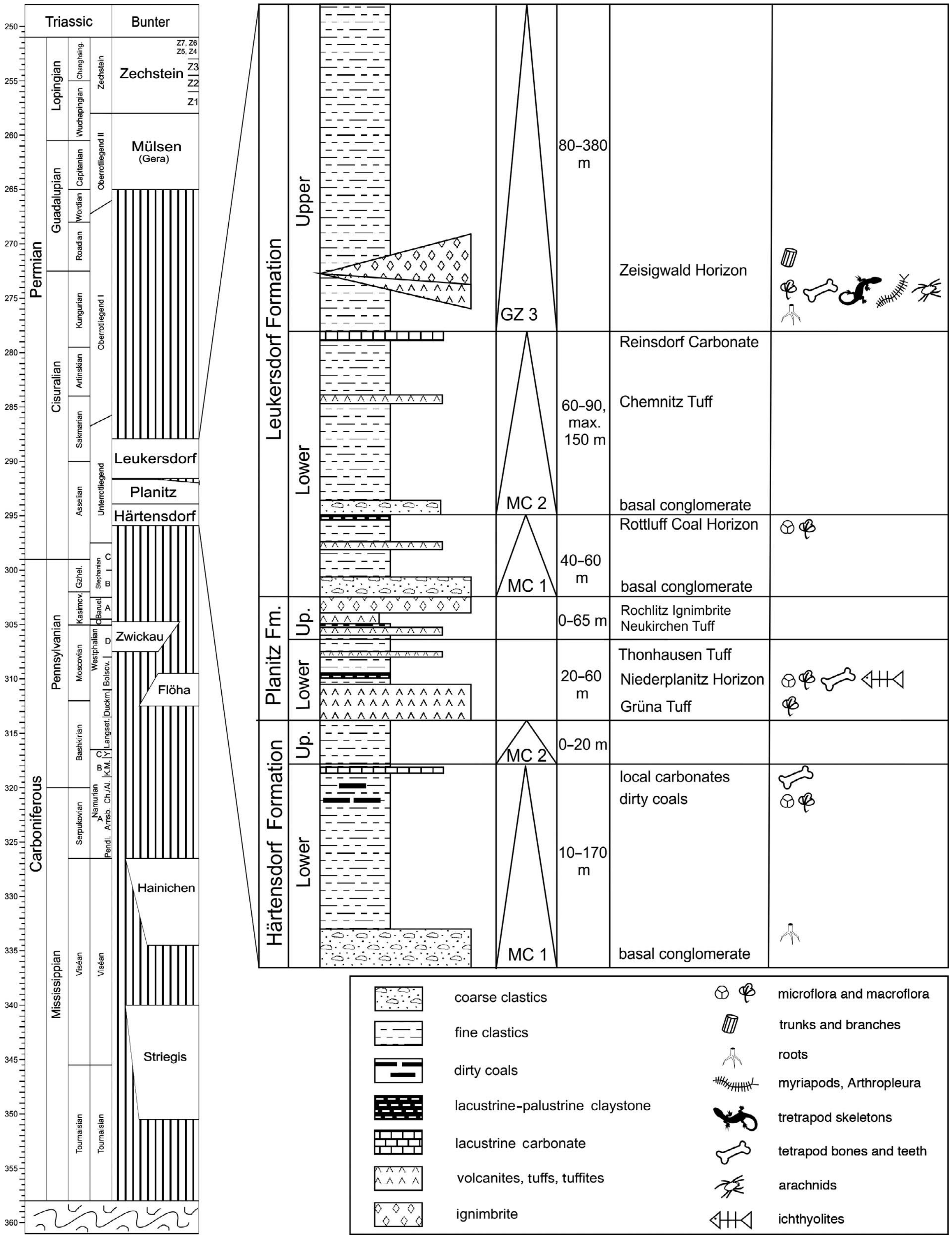

FIGURE 2—Stratigraphic frame of the Chemnitz Petrified Forest (adapted from Berger and Junghanns, 2010).

frequent dark–brown-black patches of manganese oxides and/or oxyhydrates may have been formed after the oxidation of the organic material in permeable, noncemented sediment. In contrast to the laterally discontinuous nature of the bedding at a small scale, grain-size differences may have triggered the formation of distinct soil horizons enriched in carbonates (cement, glaebules, large nodules). This differentiation, however, which was controlled by vertically directed reorganization, does not seem complete, but was interrupted several times. Both the red and purple mottling of the muddy sediment and the loss of organic matter indicate periods of soil oxidation that are usually

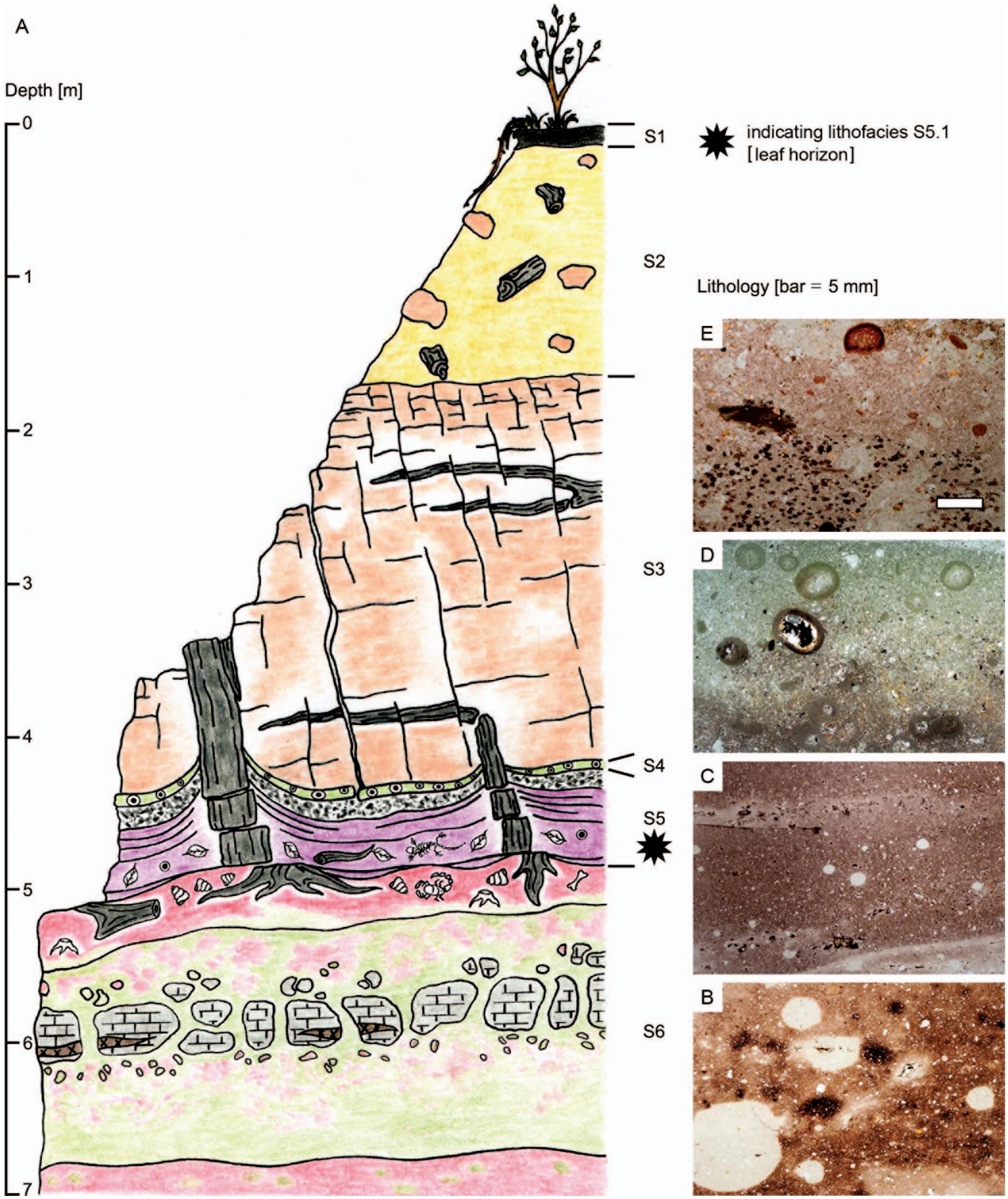

FIGURE 3—Geological section of the excavation, illustrating Units S1–S6 and their lithologies. A) Interpretative drawing. B) Unit S6 paleosol, the sedimentary base of the former forest showing rhizoliths and intense color mottling. C) Unit S5 tuff, the fine-grained material containing the majority of the compression fossil record. D) Unit S4 small sized but strongly lithified, accretionary lapilli containing layer indicating an increasing phreatomagmatic influence. E) Unit S3 coarse-grained, lapilli-rich, massive tuff deposited from a high particle concentration pyroclastic flow.

TABLE 1—Summary of the main characteristics for Units S3–S6.

	Units, facies, thickness	Lithology and structures	Fossil record	Interpretation
S3	light-red to purple-red, in places light-green lapilli-containing ash tuff >3.35 m	erosively based massive blocks with indications of reworking, poorly sorted, matrix-supported pumice clasts (altered into kaolinite), frequently accretionary lapilli green-colored bleaching zones and hydromuscovite-fluorite nodules enriched in the vicinity of petrifactions, black-colored (Mn-rich) fluid escape structures in the top of the petrified logs	Petrified trunks and branches of different order, still upright (*in situ*) standing or horizontally to oblique floating in the tuff and indicating transport direction of the flow (*Psaronius, Arthropitys, Medullosa, Cordaixylon*) rarely adpressions, casts and molds of plant axes	pyroclastic flow deposit or ignimbrite authigenic hydrothermal alteration related to early fluid mobilization from the incorporated tree trunks or branches
S4	green lithified ash tuff 1.5–8 cm	sharp or gradational based, sharply defined erosive top with different types of polygonal cracks massive to weakly horizontally stratified frequently accretionary lapilli	upright (*in situ*) standing petrified trunks (*Psaronius, Arthropitys, Medullosa, Cordaixylon*) small petrified axes (unidentified) rarely scrappy pteridophyll adpressions	deposit of a low-concentrated pyroclastic density current caused by phreatomagmatic eruption
LF5.4	light-purple-red (base) to light-grey-green (top) coarse ash tuff 13–19 cm	massive, distinctly reversely graded into bed S4 pumice lapilli, lithoclasts of quartz and micashist, feldspar crystals nonwelded	rare in fossil remains except upright (*in situ*) standing petrified trunks (*Psaronius, Arthropitys, Medullosa, Cordaixylon*)	**LF5.1–5.4** succession of ash tuffs emplaced by low-concentrated pyroclastic density currents and accompanying fallout phreatomagmatic eruption with pulsing or increasing intensity
LF5.3	purple to light-purple-red medium-grained massive ash tuff 8–9 cm	horizontal bedded, normal graded upward with less pumiceous and lithic fragments nonwelded	rare in fossil remains except upright (*in situ*) standing petrified trunks (*Psaronius, Arthropitys, Medullosa, Cordaixylon*)	
LF5.2	purple to light-grey-purple matrix-supported fine ash tuff 13–17 cm	thin horizontal bedding, repeated color and grain-size changes nonwelded initially normal graded, upward reverse graded and with laminae of pumiceous and lithic fragments	isolated petrified branches *Medullosa* terminal trunk portion with attached petioles or fronds (*Alethopteris schneideri*) in upside-down position upright (*in situ*) standing petrified trunks (*Psaronius, Arthropitys, Medullosa, Cordaixylon*)	
LF5.1	dark purple to red fine ash tuff 15–20 cm	Horizontally bedded to massive, moderately lithified, green mottled, moderately sorted nonwelded composed of several normal graded units at the base and up to three times within the whole Unit S5 horizontal muddy slickensides disrupting fossil trunks	leaf horizon with abundant plant adpressions of different size upright (*in situ*) standing petrified trunks (*Psaronius, Arthropitys, Medullosa, Cordaixylon*) complete reptile and amphibian skeletons disarticulated bones arthropods (diplopods, *Arthropleura*), arachnids (trigonotarbids, whip scorpion)	airfall tuff deposited during the first volcanic eruption's fallout
S6	red, red-brown, purple, green siltstone, limited mudstone and fine sandstone >1.85 m	structureless to weakly horizontally bedded, intensive color-mottling, muscovite containing dark brown to black-colored (Mn-rich) root impressions uppermost layer densely lithified, around rooting trunk bases carbonate-cemented areas carbonate nodules of different size, particularly enriched and associated with chert lenses, 0.8 to 1 m below the surface of S6 matrix-supported quartz pebbles	root systems of different arboreal plants (*Psaronius, Arthropitys, Medullosa, Cordaixylon*) trunk bases rooting *in situ,* preserved as petrifaction or molds-casts and as green-haloed root traces petrified deadwood trunks (unidentified), frequently impressions of plant litter terrestrial gastropods, often associated with plant roots disarticulated vertebrate bones complete scorpions in their habitat	variegated paleosol, maturity increasing with depth calcrete horizon precipitated from the groundwater

observed in well-drained surface soils. Otherwise, the gray-green mudstone with large carbonate nodules seems to be laterally persistent and reflects a high, more-or-less stable groundwater table. A horizon with very large carbonate nodules was recognized 0.8 to 1.0 m below the top surface of Unit S6. This horizon shows a gradational top and base, as well as chert lenses of authigenic silica, and is interpreted as a groundwater calcrete horizon precipitated from the phreatic zone (cf. Arakel, 1986). The lack of carbonaceous root preservation and rubefaction on one hand and evidence of periods of more sustained plant growth, waterlogging, and the lack of any endogenous ichnia on the other hand, point to a polygenetic paleosol that formed at a relatively low accommodation rate. In the end, this paleosol supported a dense vegetation dominated by hygrophilous elements, but did not develop any peat. As remnants of the primary sediment composition and structures in both the soil horizon and the sediments beneath Unit S6 indicate, soil formation and growth of the forest took place on typical Leukersdorf Formation redbeds. Deposition was dominantly by suspension, in places also with a minor bedload of sandy-pebbly braided river channels, and caused a multistacked, fine-grained deposit to form in a distal floodplain environment.

Complete root systems of the tree fern *Psaronius*, the calamitalean *Arthropitys*, and the gymnosperms *Medullosa* and *Cordaixylon* can be studied and compared for the first time from a single horizon in the Permian (Figs. 5A–F). Although these plant groups colonized the same environment and grew closely associated, they show differences in their root types and habitat adaptations. Whereas the sphenophyte *Arthropitys* has a system of woody adventitious (secondary) roots attached at an angle to its thickened stem base (Figs. 5A–B), and the tree fern *Psaronius*

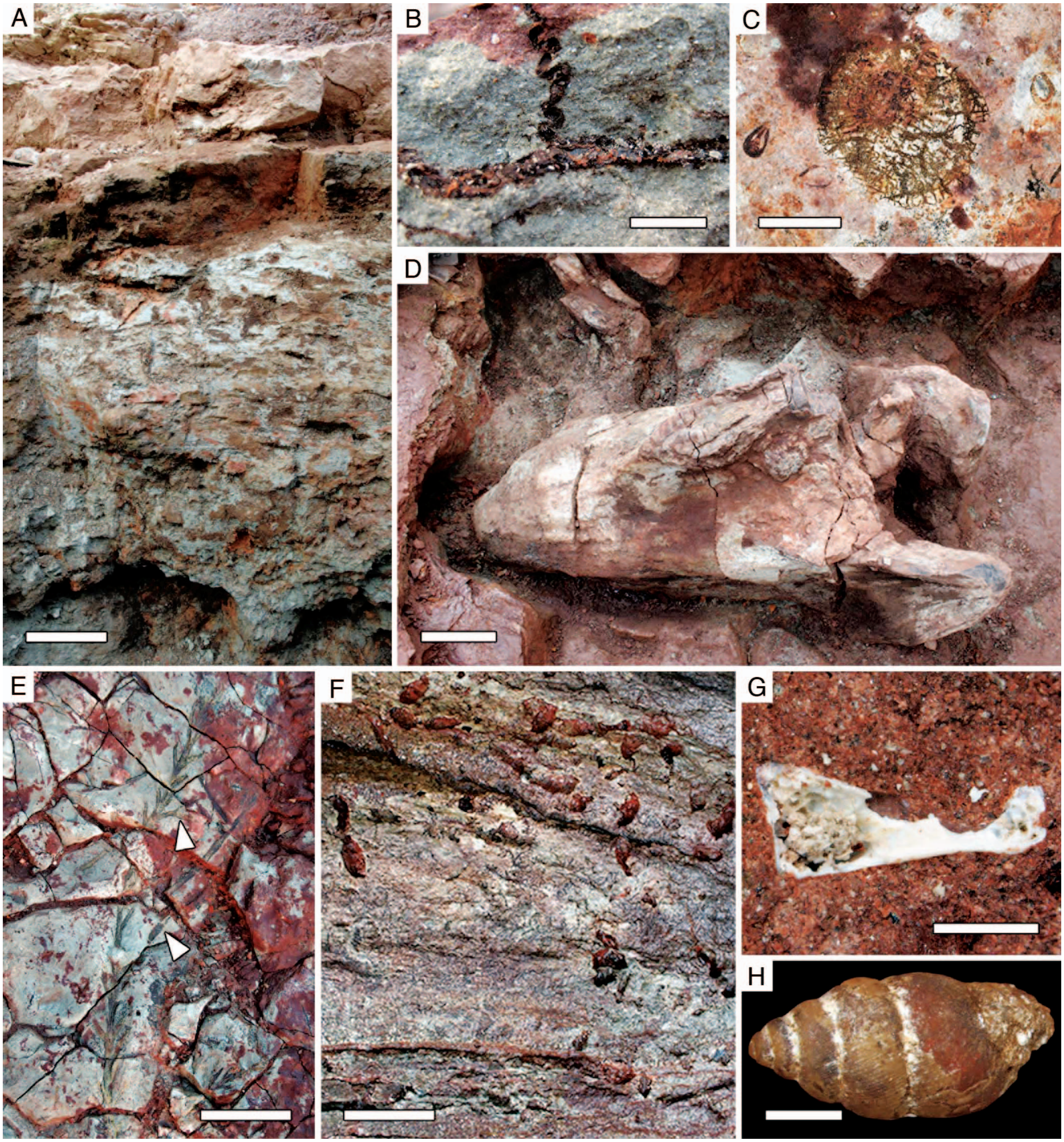

FIGURE 4—Fossil record of the paleosol (Unit S6) underlying the volcanic succession. A) Upper part of the paleosol section representing the rooting zone of the forest. Scale bar 10 cm. B) Folded vertical root in the paleosol indicating the amount of compaction. Scale bar 1.5 cm. C) Different seeds of cordaitaleans and pteridosperms as compressions on the paleosol surface (TA1024). Scale bar 1.2 cm. D) Deadwood trunk lying mainly within the uppermost paleosol and being eroded at the paleosol-tuff interface (KH0537). Scale bar 20 cm. E) Several-times-branched axis (TA0326) with loosely spirally arranged leaves (?conifer) on the paleosol surface. Branching indicated by arrows. Scale bar 10 cm. F) Gastropod casts of *Dendropupa* cf. *walchiarum* closely attached to a rhizolith in the paleosol (TA0404). Scale bar 2 cm. G) Disarticulated bone in the uppermost paleosol (TA0654). Scale 1 mm. H) *Dendropupa* cf. *walchiarum* (TA0404) from the paleosol showing permineralized preservation. Scale bar 2 mm.

shows a trunk completely enclosed by a downwardly thickening mantle of adventitious roots (Fig. 5E), the gymnosperms have orthotropic tap roots with plagiotropic lateral roots and associated fine capillary root masses (Figs. 5D, F). Detailed analysis of morphogenetic and morphologic aspects of the different root systems will provide a more sophisticated understanding of their habitat preferences and of the physiology and autecology of the parent plants (cf. Jenik, 1978).

Unit S5, Facies 5.1 to 5.4, Succession of Ash Tuffs.—Unit S5 is a thinly bedded succession of ash tuffs 0.53 m thick that can be subdivided into four different facies (Figs. 3, 6A). Facies 5.1 (bottom) to Facies 5.4 (top) are described based on a combination of lithological and paleontological characteristics. Facies 5.1 is approximately 15–20 cm thick and consists of a dark-purple, moderately sorted, fine ash tuff. Occasionally, it contains accretionary lapilli up to 5 mm and

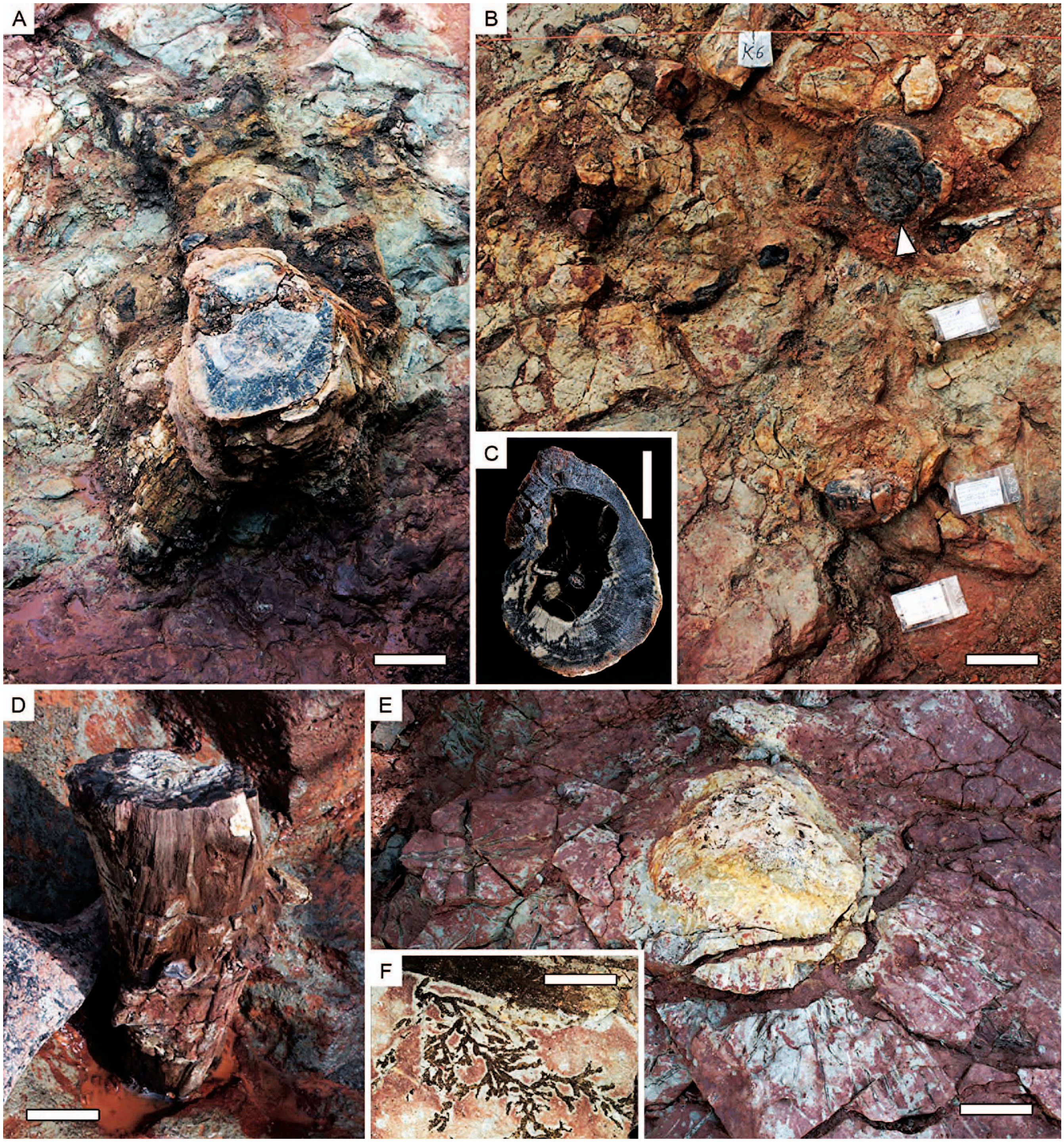

FIGURE 5—Rooting structures of the fossil forest. A) Trunk base of an *Arthropitys* calamite rooting in the paleosol (KH0042). Scale bar 10 cm. B) Roots of different size departing from the trunk base of an *Arthropitys* calamite (KH0546). Scale bar 10 cm. C) Transverse section of a root shown in Fig. 5B (arrow). Scale bar 3 cm. D) Tap root of a gymnosperm with several traces of lateral roots (KH0182-05). Scale bar 2.5 cm. E) Rooting base of a *Psaronius* tree fern in the uppermost paleosol (KH0117-04). Scale bar 10 cm. F) Small rhizoliths, several times branched, lying between large aerial adventitious roots of *Psaronius* (TA0717). Scale bar 2.5 cm.

pumice lapilli up to 1 mm in diameter. Lithic fragments (mainly mica schists) show alteration rims and reach up to 1 mm in size. Except for the lowermost 5 cm, which are thinly bedded, this facies is massive to weakly horizontally stratified with 5–10-mm-thin laminae of uneven lateral thickness. The tuffaceous matrix is nonwelded, rich in altered blocky shards up to 1 mm in size, and composed of several normal-graded units. Light-gray to green mottling frequently occurs in the vicinity of the organic inclusions. Facies 5.1 rests sharply upon a variegated paleosol and is marked by a laterally continuous slickenside of a few centimeters thickness and an infilling of dark red mud at its base. The mud appears light green in color close to organic remains, particularly to petrified plants. Depending on the local topography of the underlying paleosol, the slickenside can be traced to either the uppermost centimeters of Unit S6 or in the lowermost centimeters of Unit S5. Both strata constitute a portion of the aforementioned mud layer that was formed as a result of subrecent slope movements. The extent of these lateral movements is recognizable in every fossil trunk that still stands in growth position (Fig. 6B). Within Facies 5.1

FIGURE 6—Section at the excavation and related fossil record. A) Large upright standing petrified trunk base of a gymnosperm (KH0008) that was traced from the surface down to more than 5 m depth. Note the downward drag of several units of the section. B) Upright (*in situ*) standing trunk base of a *Cordaixylon* tree laterally dissected from subrecent slope movement (KH0073). Scale bar 10 cm. C) Upper trunk portion of an *Arthropitys bistriata* calamite, broken off and embedded upside down in the tuff (KH0294). Scale bar 8.5 cm. D) *Walchianthus* sp. male cone attached to a last-order leafy shoot of *Walchia* cf. *parvifolia* from the leaf horizon of Facies 5.1 (TA1018). Scale bar 1 cm.

horizontal slickensides are rare. The next obvious slickenside that dissects upright trunks appears at the top of this facies, and more slickensides are evident within the rest of the facies in Unit S5.

Nearly the entire adpression flora and the majority of faunal remains originate from the so-called leaf horizon, the uppermost 15 cm of Facies 5.1. The fossil content is largely confined to the lower third of this horizon; the lowermost centimeters yielded large quantities of fossil remains, except in the proximity of small upright axes, where fossil remains usually occur at higher levels inside the leaf horizon. Most leaf remains are recognizable by their curved aspect on the sediment surface as well as from sections made in different directions. In contrast to the overwhelming amount of adpression fossils, there are few horizontally oriented, petrified axes in Facies 5.1. There is a gradual or somewhat discontinuous transition between petrified and cast preservation. Within close proximity of the upright standing trunks, manganese oxides and/or oxyhydrates were precipitated, which resulted in the black staining of their green-gray haloes and cavities in the rock. Compaction-induced deformation is commonly evident in the accretionary lapilli and the upward drag of the strata around *in situ* silicified trunks (Fig. 6A).

Facies 5.2 has a gradational base and directly overlies Facies 5.1, is 13–17 cm thick, and consists of a purple to light-gray-purple, matrix-supported, fine ash tuff. It frequently contains dark-purple, compacted, deeply altered, pumice lapilli up to 12 mm in diameter that increase in frequency upward but become smaller, and green-gray to brownish lithic clasts (metamorphites with alteration rims, spherolites) up to 3 mm in size. Thin, horizontal bedding is clearly visible as repeated color and grain-size changes but slightly loses its distinctiveness upward. The tuffaceous matrix is nonwelded, initially normal graded but upward reverse graded, and contains laminae consisting of pumiceous and lithic clasts.

Whereas adpressions are rare, several detached petrified stems and branches were found. These woody axes may have been broken off and fallen down from the tree's canopy—owing to the increasing weight of falling volcanic material—and were buried in the coarse-grained tuff (Fig. 6C). Most spectacular is the terminal stem portion of a medullosan seed fern that is embedded upside down (Fig. 7A). This well-petrified, monaxial stem extends into Unit S3 and still bears two levels of helically attached fronds (Figs. 7B–E).

Facies 5.3 also has a gradational base and directly overlies Facies 5.2, is 8–9 cm thick, and shows a color transition from purple at the base to light purple to red at the top. This matrix-supported, medium-grained, massive ash tuff frequently contains dark-purple, compacted, deeply altered, pumice lapilli that are usually 1–2 mm (rarely up to 10 mm) in diameter and become rarer upward, and dark-gray to brownish, angular, lithic clasts (metamorphites with alteration rims, spherolites) 1–6 mm in size. The tuffaceous matrix is nonwelded, generally normal graded, with a decreasing frequency of pumiceous and lithic clasts upward.

Facies 5.4 has a gradational base and directly overlies Facies 5.3, is 13–19 cm thick, and shows a color transition from light purple to red at the base to light gray to greenish at the top. This matrix-supported, coarse, massive ash tuff frequently contains purple-colored, compacted, pumice lapilli that usually measure up to 10 mm (near the top rarely up to 60 mm) in diameter, and blocky shards that are 1–2 mm long; both lapilli and shards increase in frequency upward. Large ash-tuff clasts (around 50 mm) and rare accretionary lapilli that are 2–3 mm in diameter are floating in the matrix and concentrated in a narrow, ash-tuff band near the top of this subunit. Additional gray to brownish, slightly rounded, lithic clasts (metamorphites, spherolites) usually 1–2 mm in diameter (near the top rarely up to 40 mm) occur. The tuffaceous matrix is nonwelded and distinctly reversely graded into Unit S4. With the exception of upright trunks, on which this layer is stacked in the direction of the volcano, there are hardly any fossil remains in this facies.

Unit S5, Facies 5.1 to 5.4, Interpretation.—We argue that, because volcanic processes shape landscapes and affect drainage patterns, there was some relationship between the onset and increase in volcanotectonic events and the appearance of special environments retaining water that facilitated the establishment and further development of a spatially restricted habitat of plants, animals, and various interactions between them.

Unit S5, for example, may represent a half-meter succession of ash tuffs and lapilli stones that resulted from low-concentration pyroclastic density currents and accompanying fallout that was caused by an explosive magmatic to phreatomagmatic eruption with pulses of activity and a general increase in intensity. Distinguishing in detail among the different genetic types of pyroclastic deposits is usually difficult and beyond the scope of this study.

Facies 5.1 is recognized as an ash tuff that was deposited during the first volcanic fallout from a Plinian eruption. The occurrence of accretionary lapilli shows the phreatomagmatic character of this eruption that is already apparent in this very initial stage. The uppermost 15 cm of Facies 5.1 probably represent one of the most important horizons of the excavation site. This so-called leaf horizon not only contains the majority and smallest plant remains in the entire section, but also many animal remains. From the gradual increase of the transported plant fragments' size upward in the section (beginning with organic fragments, then leaves, then leafy twigs, then branches, and finally to larger trunk portions) we argue that the higher the original position of the plants in the canopy, the deeper their fragments were found in the temporal/spatial sequence of pyroclastics. Putative preeruptive leaf litter from the plant fragments broken by the initial volcanic events is difficult to distinguish, however. Further analysis of the complete adpression record will be useful for future consideration, especially to look for plant degradation effects or recognize plant remains such as conifer leafy shoots that cannot be referred to this hygrophilous habitat.

Facies 5.2 and 5.3 are comprised of thin-bedded ash tuffs that may have emplaced as air-fall or ash-cloud surge deposits. During one of these events, a *Medullosa* trunk was broken off and buried in rather coarse-grained ash tuff. This discovery provides multiple organ connections between the stem, several petioles, and pinnate fronds (Fig. 7). However, the preservation shows a gradual transition from the petrified stem, via casts of the petiole bases to foliage adpressions. Unfortunately, the preparation from the tuff is more difficult than expected and hinders the identification of the pinnae. Nevertheless, the leaf type (Figs. 7D–E) is comparable to *Alethopteris schneideri*, a frequent seed fern taxon in the Rotliegend of Saxony (Barthel, 2006 in 2003–2008), which has been repeatedly noted in close proximity of this *Medullosa* stem. Since little is known about ontogenetic variation in *Medullosa* stems, our new find cannot be referred to one of the published species of this arborescent seed fern (Weber and Sterzel, 1896). Hence, we can only describe this specimen as an upper trunk portion that reflects a relatively young ontogenetic stage, characterized by a wide pith with numerous small and very regularly arranged, sometimes forking vascular bundles, each showing little secondary growth and a narrow outer ring of secondary tissues (Figs. 7B–C). The question of whether this anatomy represents a new species or simply reflects the upper stem portion of a *M. stellata* trunk must remain open at this time.

Later, in subrecent times, fine-grained laminae of the tuff succession may have facilitated the formation of the horizontal slickensides that resulted in the multiple shears of upright-standing plant axes (compare with Fig. 6B).

Facies 5.4 is interpreted as a deposit that settled from a dilute pyroclastic suspension current, based on its depositional features. This unit is extremely poor in fossil remains, which makes the interpretation difficult.

Unit S4, Lithified Accretionary Lapilli-Rich Tuff.—Unit S4 overlies Facies 5.4 and has a gradational base. The thickness of Unit S4 varies between 1.5 and 8 cm, and the strong lithification is one of its most striking characteristics. This unit has a wavy top, and its thickness is raised in depressions, but reduced on both elevations and around upright standing trunks. The pale-green to dark-green (sometimes purple-red), fine ash tuff is matrix supported and massive to weakly horizontally stratified. Unit S4 could be subdivided into two zones. The lower zone, nearly one third of the thickness, is dominated by white, blocky, pumice lapilli up to 4 mm in diameter, while the remaining upper zone is dominated by accretionary lapilli, floating in a fine tuff matrix of devitrified vesicular shards. Accretionary lapilli average 5 to 6 mm (rarely to 10 mm) in diameter, and show a core of coarse-grained ash surrounded by a multilayered rim of the finest, normally graded ash. Crystals, blocky shards, and lithic fragments have been recognized as the nuclei of the accretionary lapilli. The nuclei are surrounded by shard-dominated, nonwelded ash material found elsewhere as the matrix of this unit.

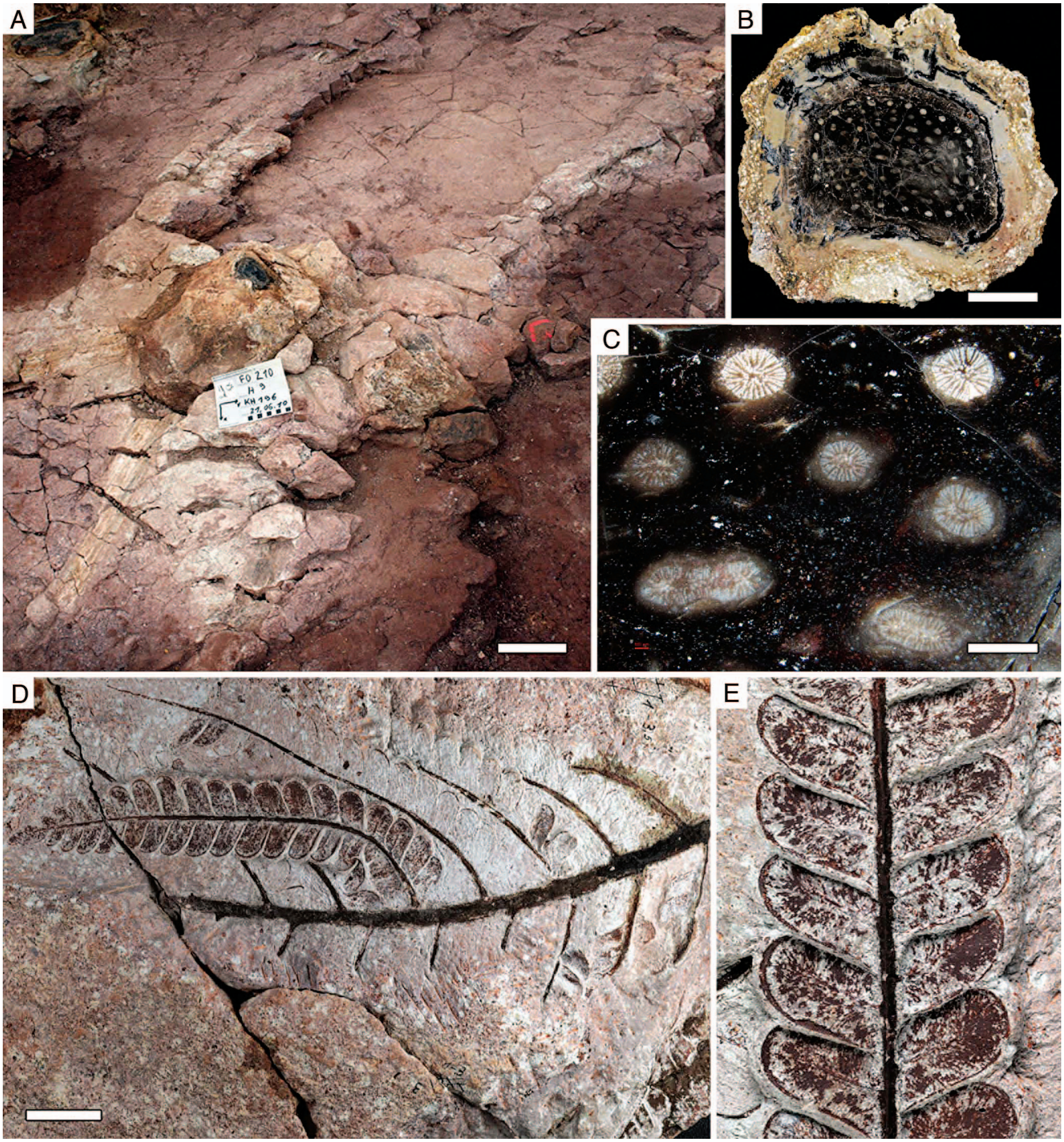

FIGURE 7—*Medullosa* trunk showing organ connections A) Terminal trunk portion with attached fronds, deposited in upside-down position of Facies 5.2–5.3 (KH0196). Scale bar 15 cm. B) Transverse section of the *Medullosa* stem shown in view A. Note the regular arrangement of the many vascular bundles in the pith. Scale bar 2.5 cm. C) Detail of view B showing circular to elliptical-shaped vascular bundles. The lowermost two bundles show lateral enlargement close to bifurcation. Scale bar 3 mm. D) Part of the frond attached to the *Medullosa* stem showing *Alethopteris schneideri* pinnae. Scale bar 2.5 cm. E) Detail of the pinnules, their alethopterid attachment to the pinna axis and venation.

Accretionary lapilli are sometimes slightly compacted or broken, but still recognizable as fragments. Additionally, up to 1 mm large lithic fragments occur. Unit S4 is limited by a sharply defined top that exhibits different types of polygonal cracks (Fig. 10D and Rößler et al., 2009).

Fossil remains are rare in this unit. The emplacement of isolated cordaitalean and pteridosperm leaf fragments often shows an unusual inrolled appearance and edgewise burial in this thin unit. A few small petrified axes were also found in horizontal position.

Unit S4, Interpretation.—This thin but distinctive lithified unit clearly indicates increasing phreatomagmatic influence. The deposit contains shards showing shapes typical of both explosive magmatic and phreatomagmatic fragmentation processes. An increase in the occurrence of accretionary lapilli accounts for the presence of suspended ash and moisture in a subaerial environment (cf. Schumacher and Schmincke, 1991). Accretionary lapilli are commonly present in ash-grain-size fall deposits, and the considerable portion of broken accretionary lapilli could point to a fall deposit like an ash cloud that often accompanies pyroclastic flows. The sum of textural characteristics, such as poor sorting and variation in thickness of the unit, however, also argues for a deposit that resulted from a low-concentration pyroclastic density current. The sum of features recognizable at the top of Unit S4 (Fig. 10D) shows that the ecosystem was nearly destroyed during its deposition. Only a few large trees extended into Unit S3 and, therefore, resisted the depositional processes up to this stage.

Unit S3, Lapilli-Containing Ash Tuff.—Unit S3 overlies Unit S4 with a sharp erosive base and reaches a preserved thickness of 3.35 m. The influence of surface weathering, resulting in the gradational disaggregation of the rock near the top of Unit S3, is obvious. The purple-red ash tuff is massive to thick-bedded, matrix supported, and rich in compacted to elongate pumice lapilli that are usually alterated into clay minerals and vary in diameter from 15 to 50 mm. In some catchment areas, upright standing petrified trunks and broken branches retain pumice blocks up to 200 mm in diameter. Furthermore, the matrix frequently contains spherical to ellipsoid accretionary lapilli up to 12 mm in diameter, which seem to be stronger lithified than the nonwelded tuffaceous matrix and, therefore, better resist weathering. Scattered angular lithic clasts (biotite, mica schist), up to 3 mm (rarely to 9 mm) in size, occur. The basal layer of Unit S3, up to 30 cm thick, shows frequent indications of Cenozoic gravity-driven shear. Vertically oriented cracks of decimeter size dissect the rock of Unit S3 affecting the preservation of the plant fossils. Unit S3 contains abundant, horizontally positioned petrified stems and branches; some of the thicker trunks that resisted volcanic emplacement processes that occurred below this level, remained upright (Fig. 9B). The horizontally embedded stems are oriented more or less in east-west direction, the top of the trees pointing westward, except when they got stuck on other still-upright-standing trunks. This direction likely indicates the major direction of the eruption of the pyroclastics. One exception to the aforementioned directionality is a cordaitalean trunk with attached branches of different lengths arranged in several vertical tiers (Fig. 9A). This trunk is oriented in the opposite direction as the stems in this unit, but its branches are bent into the direction of the pyroclastic flow.

There is a spectrum of pale-green bleached zones that are commonly associated with embedded petrified axes, regardless of whether they had been embedded upright, in growth position or horizontally (Figs. 10A, C–D). A 3.4 × 4.2 m large bleached area of repeated distinct green-colored rims surrounds one of the upright trunks with a diameter of 40 cm. The horizontal petrified stems always tend to be situated in the lower part of the bleached halo; the halo can extend up to 1 m above the fossil stem. Within these bleached zones, the rock is often stronger lithified, showing reduced compaction, which more likely reflects the primary texture than the nonbleached areas. The center of the catchment areas, where the lithification of the tuff matrix is strongest, not only still shows the original texture and structure of the rock, but the lack of permeability preserved calcium carbonate and prevented the infiltration of the dark-brown to black manganese oxides and/or oxyhydrates that are frequently observed elsewhere in the green bleached areas around petrified stems and branches.

Unit S3, Interpretation.—Unit S3 is interpreted as a primary pyroclastic flow deposit with a high concentration of particles resulting from a phreatomagmatic eruption. This is evidenced by a variety of criteria that characterize deposits of high-concentration pyroclastic density currents (Druitt, 1998; Branney and Kokelaar, 2002). Among these criteria, we recognize in Unit S3 textural and such facies characteristics as poor sorting, from massive to graded and diffusely stratified with a sharply defined erosive base. Additionally, the rock exhibits multiple indications of directional flow. In some cases, the buckling of branches is exceptionally well preserved (Fig. 9D). Tree trunks and branches are frequently broken off, and, if still attached, they are preserved with their apices pointing westward. Whereas the basal part of this unit bears small-sized stems and branches, the axes become larger in diameter toward the upper part of the unit.

Although the matrix remains nonwelded, Unit S3 seems to be columnar jointed. This type of structure, which usually results from contraction during the cooling of primary hot emplaced pyroclastics, is visible in the form of large-scale polygonal cracks on the Unit S4–S3 boundary (Fig. 10D). These cracks, which imply primary emplacement of the massive rock, transect it perpendicular to the conspicuous foliation caused by compacted, elongate pumice fragments. Primary hot emplacement is also indicated by fluid-escape structures frequently observed above tree trunks (Figs. 10B, E), indicating heat-mobilized fluids arising from the plant tissues. Fluid mobilization from the trees may also be underlined by the grain-size distribution and geochemical behavior along the upward-directed escape structures (see Figs. 10B, E). Another distinctive pattern that reveals the distribution of the former plant's fluids into the sediment is seen in the frequently occurring bleached zones close to the petrified stems and branches. In 3D space, mushroom-shaped, bleached areas outline the petrified trunks and branches, and commonly widen in the space above them (Fig. 10C), and considerably differ from the polydirectional distribution of the bleaching haloes found around organic material included in sediments as, for instance, visible in the paleosol, Unit S6. In addition, preliminary results from the geochemical composition of the tuff matrix indicate some kind of autometasomatic reactions in the upper periphery of the fluid-delivering stems or branches and most likely point to an authigenic hydrothermal alteration. The periphery of nearly all petrified trunks and branches shows a pattern of spherical mm-sized cavities, either empty or kaolinite filled, and sometimes rimmed by straight edges that may have been formed during mineral growth (Fig. 10F). Hence, cortex preservation in the woody plants is rather rare, since the periphery of their stems seems to be strongly affected by the hot ignimbrite. In some cases, thin cortex layers remain in the rock, while the xylem core of the stems easily breaks off during preparation.

In the lowermost centimeters of Unit S3, close to the top of Unit S4, many small, upright plant axes are abruptly truncated, because they were cut by the shearing power of the emplacing Unit S3 density current.

FOSSIL RECORD OF THE SECTION

To get an overview of the heterogeneous finds, fossil specimens were sorted into different categories and characterized as follows:

Categories A, B, and C of petrified stems are established to distinguish them with regard to their information potential for future reconstructions of the fossil plants. Category A trunks were found rooted in place, and information from their site of growth and plant community structure is possible to extract. Category A trunks represent a unique, unprecedented opportunity to evaluate community density and spatial heterogeneity in the Chemnitz fossil forest in the future (Figs. 10A, D).

Category B trunks are comprised of upright trunk bases that are broken off, or of large-scale trunks that exhibit branching patterns, which allow for the reconstruction of the growth architecture in any part of the plant (Figs. 9A, 11A).

Category C trunks are all remaining detached parts of petrified trunks or branches, freely floating in the tuff matrix. This material does not offer any information about the original place of growth of the parent plants, although they provide taphonomic data on volcanic emplacement and transport processes (compare with Fig. 6C).

In some places, especially in the lower strata beneath S4, petrified organs grade into casts and appear more compressed. There are in some cases certain gradations between different preservational forms, such as between petrifactions and flattened casts without any organic material left, but with mineral matter or tuff that replaced the organic substance.

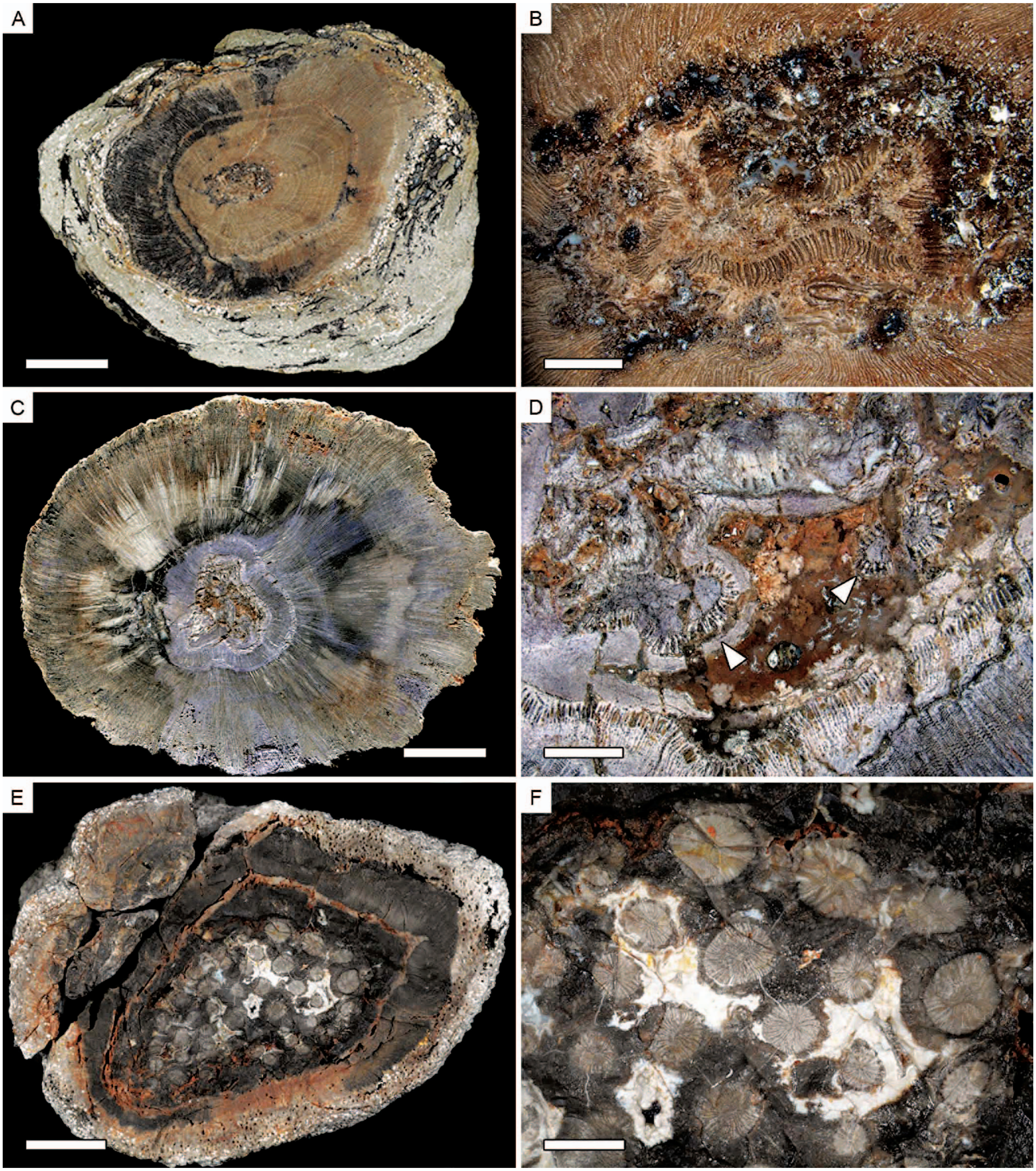

FIGURE 8—Anatomical diversity of medullosan seed ferns at the excavation. A) Transverse section of a *Medullosa*-like stem showing a small pith, limited secondary growth in centripetal direction but extended secondary growth in centrifugal direction (KH0286). Scale bar 2 cm. B) Detail of view A. There is probably no further vascular bundle inside the pith. Scale bar 2.5 mm. C) Transverse section of a *Medullosa stellata* f. *lignosa* stem showing small pith and extended secondary growth (KH0067). Scale bar 3 cm. D) Detail of view C showing small circular-shaped vascular bundles in the pith (arrow). Scale bar 2.5 mm. E) Transverse section of a *Medullosa stellata* stem showing a large pith with numerous vascular bundles surrounded by a woody ring (KH0056). Scale bar 3 cm. F) Detail of view E showing vascular bundles of different size in the pith. Scale bar 1 cm.

Petrified Fossils

The majority of the most instructive excavation finds are petrified trunks, axes, and branches showing various orders of branching. They are mostly silicified or preserved by purple calcium fluoride, rarely calcified, and give us 3D insight into the cellular detail of arborescent plants and their organs. Among them are psaroniaceous tree ferns that until the present study, were thought to be exclusively those of the distichous branching type, calamitaleans of the *Arthropitys*-wood type, medullosan seed ferns with a conspicuous anatomical diversity (Fig. 8),

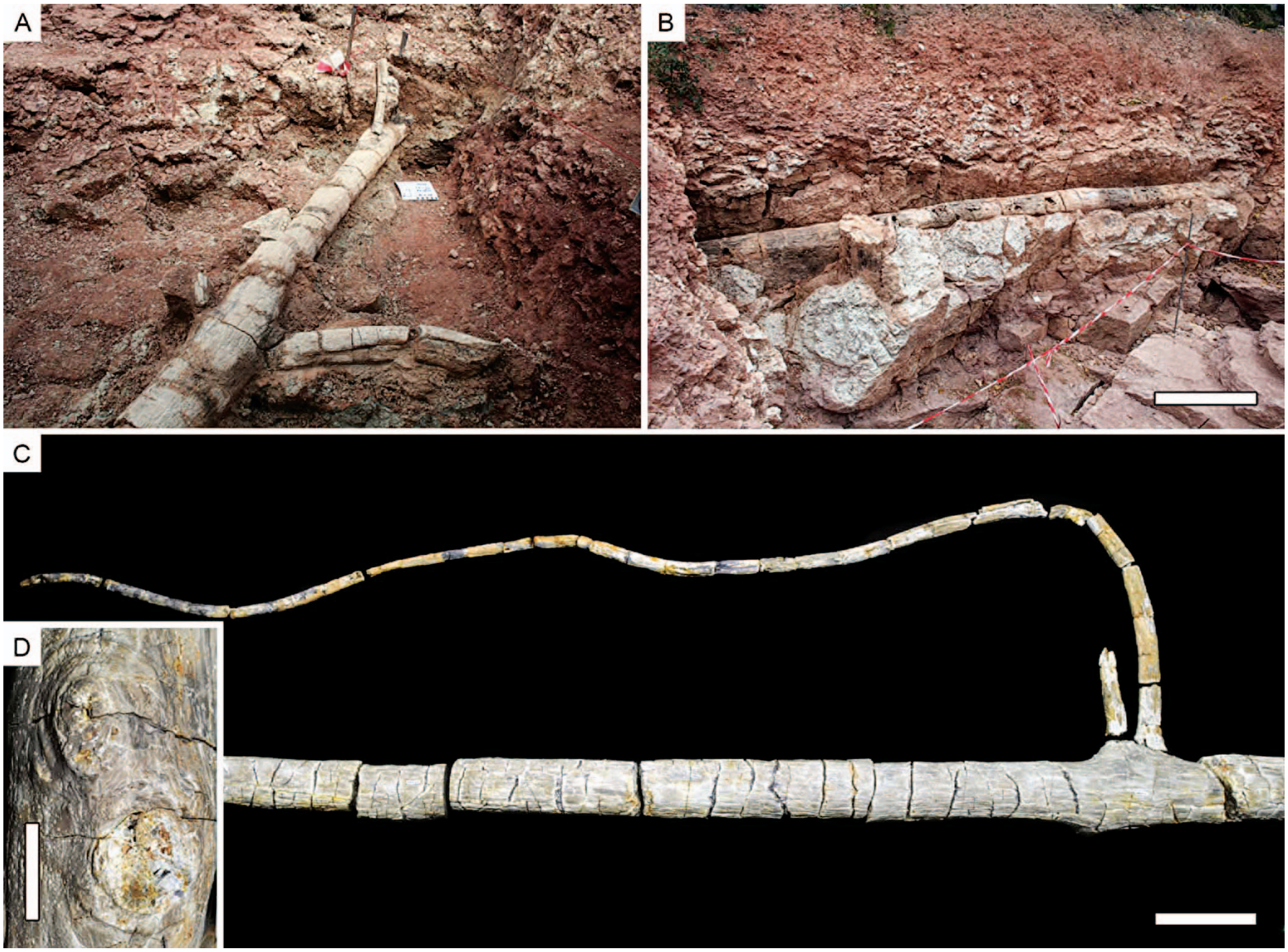

FIGURE 9—Preservational diversity of cordaitaleans at the excavation. A) *Cordaixylon* trunk with attached branches up to 3 m long embedded in the Unit S3 pyroclastic flow deposit (KH0021). B) Gymnosperm trunks in the northernmost part of the excavation area; the one in front is still standing *in situ* (KH0004), the one behind lies horizontally in the Unit S3 ignimbrite (KH0025). Scale bar 1 m. C) *Cordaixylon* stem with attached branches. Surface sandblasted (KH0073). Scale bar 20 cm. D) Detail of the specimen shown in view C with branch traces. Scale bar 4 cm.

and gymnosperms of cordaitalean affinity. Petrified conifer remains are rare and buried not *in situ*. Many of the 53 aforementioned specimens represent basal stem portions of different sizes that are still standing upright in their growth positions and rooted in the underlying paleosol. The preservation of the stems generally worsens the closer one gets to their respective root systems, which are located significantly beneath Unit S4, except for the root-emanating stem bases of the larger trees and deadwood trunks in Unit S6. Although many petrifactions exhibit anatomical preservation, the rarity or absence of organic material has resulted in weak contrast in the plant tissue, which unfortunately complicates the recognition of diagnostic details of taxonomic value. Plant remains preserved in fluorite are often destroyed or poorly fossilized. There is no fluorspar beneath Unit S4, however. Nevertheless, we anticipate the future chemical dissolution of fluorspar from the petrifactions (Fig. 11F). Rooted trunk bases, such as in calamite KH0042, show decimeter-long cavities (Fig. 5A) that are definitely too large to occur in an upright, living tree. Instead, the cavities may be related to previous infilling by fluorite, but this needs further research.

The most complete and significant preservation of petrified material was traced in the ignimbrite of Unit S3. An exceptionally large calamite bears a crown that is repeatedly branched and estimated to have been at least 15 m in height with at least three orders of secondary woody appendages that formed a large crown (Figs. 11A–C). This find provides insights into both the spatial arrangement of the complex branching system and anatomical details of the calamite. This is the first time that the branching architecture of an anatomically preserved calamite tree is clearly discernable in three dimensions. This peculiar architecture demonstrates that this Permian calamitalean developed a complex branching pattern. In combination with the thick woody trunk consisting of a major parenchyma portion, frequent growth rings, and many branch scars, this type of growth also indicates that some calamitaleans could survive episodes of environmental stress, possibly by shedding their leafy branches (Rößler and Noll, 2010). This suggests that the plasticity inherent to some calamitaleans enabled different growth strategies in the face of environmental changes and in competition with the neighboring ferns and gymnosperms. Depending on the degree of silicification, the quality of preservation can differ considerably. Sometimes small and dispersed organic remains, which were altered into anthracite during fossilization (cf. Nestler et al., 2003), or the selective enclosure of dark-purple fluorite are useful for recognizing cell wall features, such as diagnostic wall thickenings or pitting (Fig. 11C). The minor portion of remaining organic constituents, however, does not justify calling the specimens permineralizations. Although petrifactions are more likely to be poorly preserved in both the Units S4 and S5, paleosol Unit S6 contains many well-preserved, silicified remains, which include both upright *in situ* rooted tree bases and horizontally positioned deadwood logs (Figs. 3E, 5A, 5D).

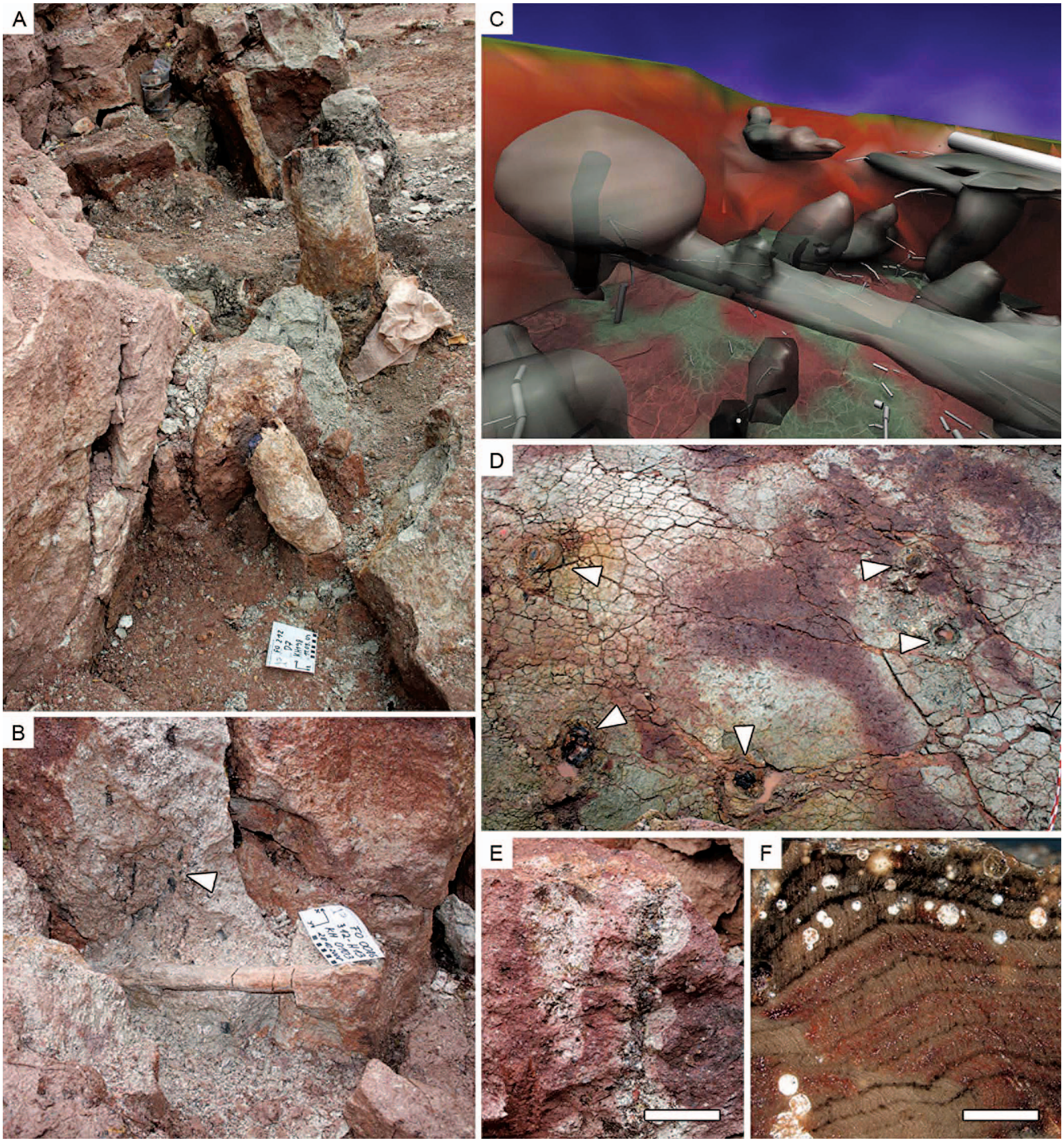

FIGURE 10—Plant taphonomic features related to volcanism. A) Southern part of the excavation area showing several upright-standing trunks indicating vegetation density in the environment. B) Petrified gymnosperm stem surrounded by coarse-grained, green-gray bleached tuff. Note the vertical black-colored fluid-escape structures departing from the top of the stem (KH0103). C) Three-dimensional model showing excavated stems and branches and the spatial extension of the bleaching haloes surrounding the petrifactions. D) Unit S4 surface showing several trunk bases and different types of cracks in the rock. Note the bleaching haloes around the trunks. E) Fluid-escape structures visible by black-colored vertical structures and their green-gray haloes. Scale bar 10 cm. F) Trunk periphery of an *Arthropitys bistriata* calamite with extended secondary growth exhibiting six- to eight-sided holes of millimeter size filled with kaolinite (KH0052). Scale bar 3 mm.

Adpression Flora and Fauna

During an early stage of volcanic activity, volcanic ashes were deposited and covered the standing vegetation. As a result, many trees shed their leaves, which are found embedded in a fine-grained ash-tuff layer near the basis of Unit S5, Facies 5.1. In comparison to clayey-silty epiclastics, the pyroclastics responsible for incorporating the plant material are relatively coarse and consist of angular fragments. Fine details of diagnostic features like venation patterns or delicate foliage types are, therefore, often not well preserved. In contrast, such small but robust plant remains as conifer twigs (*Walchia piniformis, W. parvifolia*), or robust cordaitalean or pteridoperm leaves (e.g., *Taeniopteris abnormis*), appear sufficiently well preserved (Fig. 6D). Since the plant fossils are exclusively adpressed in the tuff, organic

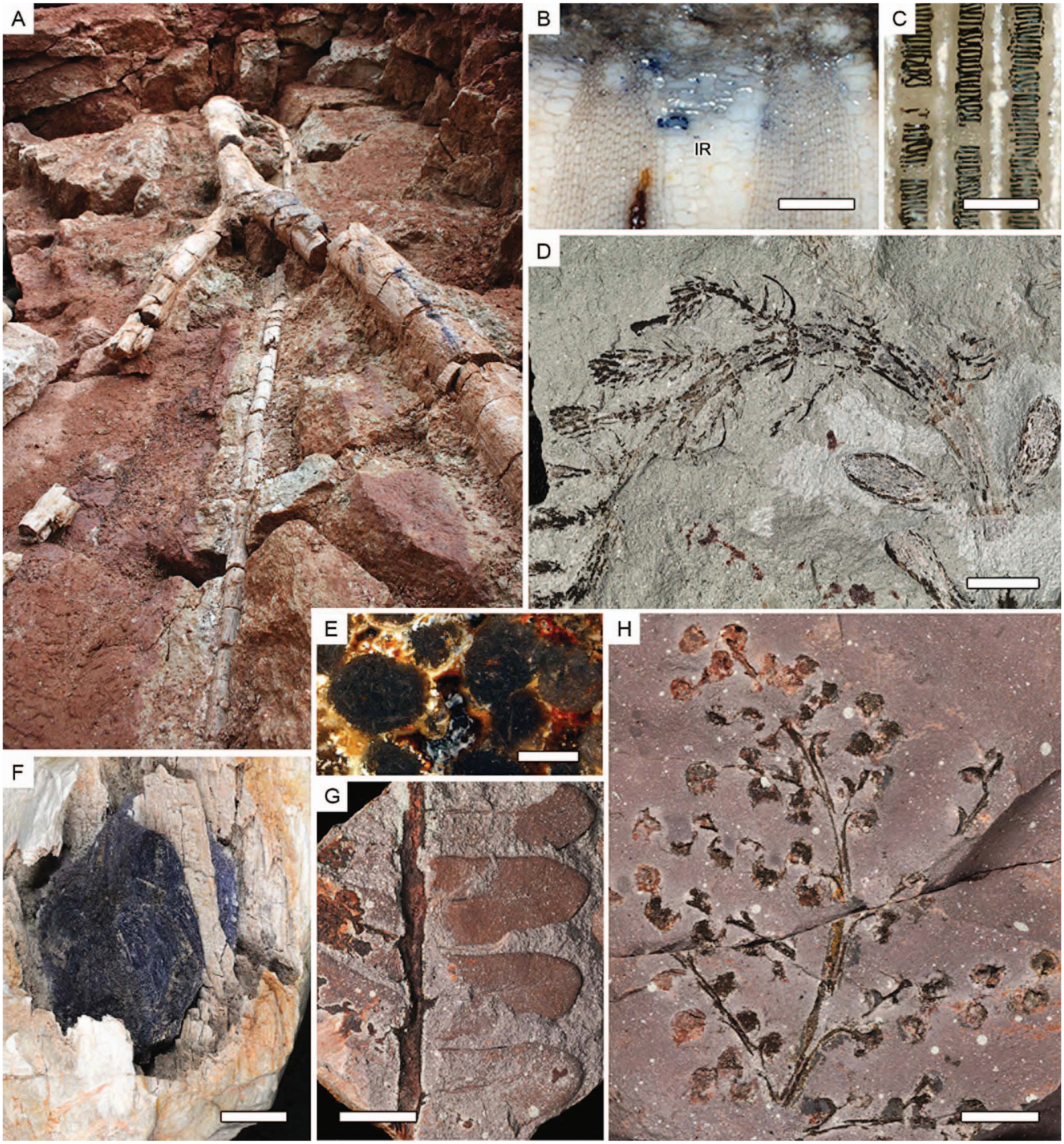

FIGURE 11—Diversity of the plant fossil record. A) More than 10-m-long *Arthropitys bistriata* tree showing different order branches (KH0052, KH0054, KH0057, KH0058, and KH0072). B) Anatomical preservation of the calamite tree of view A showing two initial vascular segments with carinal canals separated by an interfascicular ray. Scale bar 500 µm. C) Radial section of secondary xylem tracheids showing scalariform wall thickenings. Scale bar 100 µm. D) *Annularia spicata* shoot with juvenile leafy lateral twigs. Scale bar 1 cm. E) Large-sized coprolites found in the pith of the calamite figures in view A. Scale bar 2 mm. F) Petrifactions found in Unit S3 ignimbrite show selective preservation as fluorite. Scale bar 1 cm. G) *Neurocallipteris planchardii* pinnae, frequently found close to medullosan seed fern stems (TA0827). Scale bar 1.5 cm. H) Putative pteridosperm fructification 3D preserved in fine-grained tuff of the leaf horizon (TA0164). Scale bar 1.5 cm.

remains are lacking. We, therefore, have neither a classical compression flora nor an impression flora such as those that we have found in coeval claystones and siltstones. Our material hardly shows any filmy venation; between the upper and lower side of the impressions, there is only crumbly, brownish material that replaced organic remains (Figs. 11D, G–H). In contrast to classical adpressions, our fossil material additionally reveals 3D aspects to some degree.

Among pteridosperm foliage *Neurocallipteris planchardii* and *Alethopteris schneideri*. are frequent in tuffs in the Chemnitz Basin and usually described as fronds of medullosan seed ferns (cf. Taylor et al., 2009). We now know that the classical material of *Alethopteris schneideri*, published by Sterzel (1918) under the name *Callipteris weberi* (see Barthel, 1976), came from the same horizon, Facies 5.1 of Unit S5. There are still a few nicely preserved pteridosperm reproductive structures that remain unidentified (Fig. 11H). Shoots with pteridosperm reproductive structures even show some 3D structure in the tuff, but lack any organic material.

Psaroniaceous tree ferns were also recognized in the adpression flora. Unfortunately, with the exception of a few petiole bases, foliar remains in organic connection are not known. The pinnae of *Lobatopteris geinitzii*, however, have several times been found in the proximity of the aforementioned distichous *Psaronius* trunks.

With regard to *Arthropitys bistriata* stems, the only potential candidate that could represent the associated foliage of these frequently found stems is *Annularia spicata* (Fig. 11D). This type of foliage was frequently found in close proximity to *Arthropitys bistriata* stems (TA0565). This association is confirmed by the historical collection in the Museum für Naturkunde Chemnitz and suggests a correlation between this small-leaved *Annularia* and *Arthropitys bistriata*. We cannot exclude, however, that this fossil species could have had different types of leafy shoots.

Along with leafy shoots, pinnate fronds, detached whole and fragmentary leaves, the leaf horizon has yielded the first outstanding faunal remains. The latter include such vertebrates as several reptile skeletons, aistopod microsaurians, and remains of an eryopid amphibian, as well as such invertebrates as diplopods, *Arthropleura* remains, various arachnids like a whip scorpion, and trigonotarbids (Fig. 12). Faunal remains are described in detail by a series of papers that will start with the youngest record of the Trigonotarbida to date (J. Dunlop and R. Rößler, unpublished data, 2012).

With increasing volcanic activity, more twigs and branches were broken off from trees and deposited. Such conifer remains as leafy twigs, pollen cones, and small branches were apparently transported by storms from adjacent areas to the basin, where they are now found in the lowermost pyroclastic Unit S5 (Fig. 6D). Kerp et al. (1990) proposed wind transport of remains of Walchian conifers into the depositional basin. No conifers, however, were recognized among the *in situ* preserved suite of trunks and axes at Chemnitz.

DISCUSSION

The Permian represents a crucial time in the evolution of plants and terrestrial ecosystems in particular (Kerp, 1996; Barthel, 2003–2008; DiMichele et al., 2006; Montañez et al., 2007). In Chemnitz, an early Permian forest was buried in growth position and as a so-called T^0 assemblage (cf. DiMichele and Falcon-Lang, 2011). In contrast to previous work, emphasis here is placed on a very detailed data acquisition, offering the possibility to plot the position and orientation in a 3D network with centimeter accuracy. The fossils and associated data will allow the application of various approaches, not only with regard to paleontology and paleoecology, but also to the mineralogy and volcanology. As reconstructions of fossil forests indicate, there is a growing awareness of the high potential to interpret 3D data obtained from the mapping of T^0 assemblages. A Upper Jurassic Araucariaceae-dominated forest from Northwest China (Hinz et al., 2010), a Pennsylvanian coniferopsid forest from New Mexico, United States (Falcon-Lang et al., 2011), and a series of ancient coal forests preserved in the Pennsylvanian of Bohemia (Opluštil et al., 2009) contribute to the knowledge of plant diversity, spatial density, canopy appearance, and paleoecological gradients in various paleoenvironments.

Our fossil record provides an excellent opportunity to investigate an *in situ* hygrophilous habitat that was buried instantaneously after a series of successive volcanic eruptions. Presented finds and data give particular insights into a diverse ecosystem. Not only fossil-rich plant assemblages, but also a number of animal remains and interactions between the organisms were preserved by pyroclastics (Fig. 11E). This offers the unique opportunity to reconstruct the most complete Permian forest ecosystem known to date. By studying the large tree trunks, their rooting systems, petrified branches, and the many other plant and animal remains found in close proximity, we will have the chance to present more realistic reconstructions of plants and their habitat and to decipher the paleoecological framework in more detail than ever before.

The *in situ* plant community, recognized at the excavation site, consists of several species of psaroniaceous tree ferns, calamitaleans, medullosan seed ferns, and cordaitaleans. We consider significant that both the aerial parts and the rooting systems of the former plants were documented from a single bed. While cast-preserved *in situ* fossil forests of the aforementioned plant groups were reported several times from Pennsylvanian age clastics (Gastaldo et al., 2004; Falcon-Lang, 2006), anatomically preserved specimens remain rare (Ehret and Phillips, 1977). In contrast to the classical descriptions and figures provided by Grand'Eury (1877) with regard to the rooting bases of calamitaleans, we can contribute some new observations that differ fundamentally. There is ample evidence that *Arthropitys bistriata* trunks produced a network of surface roots. They may have arisen as adventitious roots from thickened basal trunks anchoring them in the upper soil horizon. Each of the roots can show considerable secondary growth, and as with the aerial woody stems and shoots, they also reflect growth interruptions. At first glance they much resemble extant woody trees, and they have nothing in common with the popular reconstructions of any underground rhizomatous system (Fig. 5A). As early as shown by Grand'Eury (1877) the calamitaleans appear as single trees, but in contrast to the examples from the Carboniferous of France, their stem abruptly ends close beneath the soil surface, only the roots penetrate deeper into the sediment. This evidence corresponds to previously made observations for *Arthropitys* calamitaleans from the Permian of Tocantins, Brazil (Rößler, 2006).

Although our excavation highlighted only a detail of the former habitat, the species composition evidenced among arboreal taxa is interpreted as a typical plant community found in Late Pennsylvanian and early Permian wetland environments, in its total diversity comparable to many other occurrences of this time span in Europe (Galtier et al., 2011; Barthel and Rößler, 2011), in North America (DiMichele et al., 2004), and even in northern Brazil (Rößler, 2006).

There is a diversity of preservational types including some transitional forms, which are not reflected in the literature so far. In addition to petrifactions, there is a special type of adpressions of plant organs in ash tuff, sometimes still reflecting 3D aspects, although tiny structures of the leaf surface largely remain hidden. A considerable portion of this material shows juvenile organs, organ connections, or clearly reflects various ontogenetic stages of the plants. We documented casts of different size made of mineral material or fine ash tuff, but also well preserved specimens that reveal microscopic structures in the plants' internal anatomy. Most of them are preserved as siliceous or fluoritic cellular petrifactions. Depending on the amount of remaining organic constituents and the completeness of tissue mineralization, the quality and fidelity of preservation can differ considerably, and is not as excellent as in many true permineralizations (Feng et al., 2011). Chert lenses are many times reported from volcanic successions (Trewin, 1994; Galtier et al., 2011), and often they are known for their exceptionally well-preserved fossil record (Rex, 1986; Krings et al., 2011). Some of them were found in the paleosol, Unit S6. While this horizon provided such diverse fossil remains as leaves, roots, gastropods, and bones (Figs. 4B–H), the few investigated cherts were unfortunately unfossiliferous.

A first appraisal of all observations enables us to reconstruct the volcanic and taphonomic processes and their chronology. We obtained multiple indications of the emplacement directions of the air-fall tuffs and pyroclastic flow deposits. This will enable us to estimate the influence of depositional events on standing vegetation. The ecosystem was nearly destroyed during the deposition of Unit S4. Indications of survival, regeneration, and recolonization are lacking until now. The surface of Unit S4, however, provided several vegetation-induced sedimentary structures (VISS *sensu* Rygel et al., 2004), such as mounds

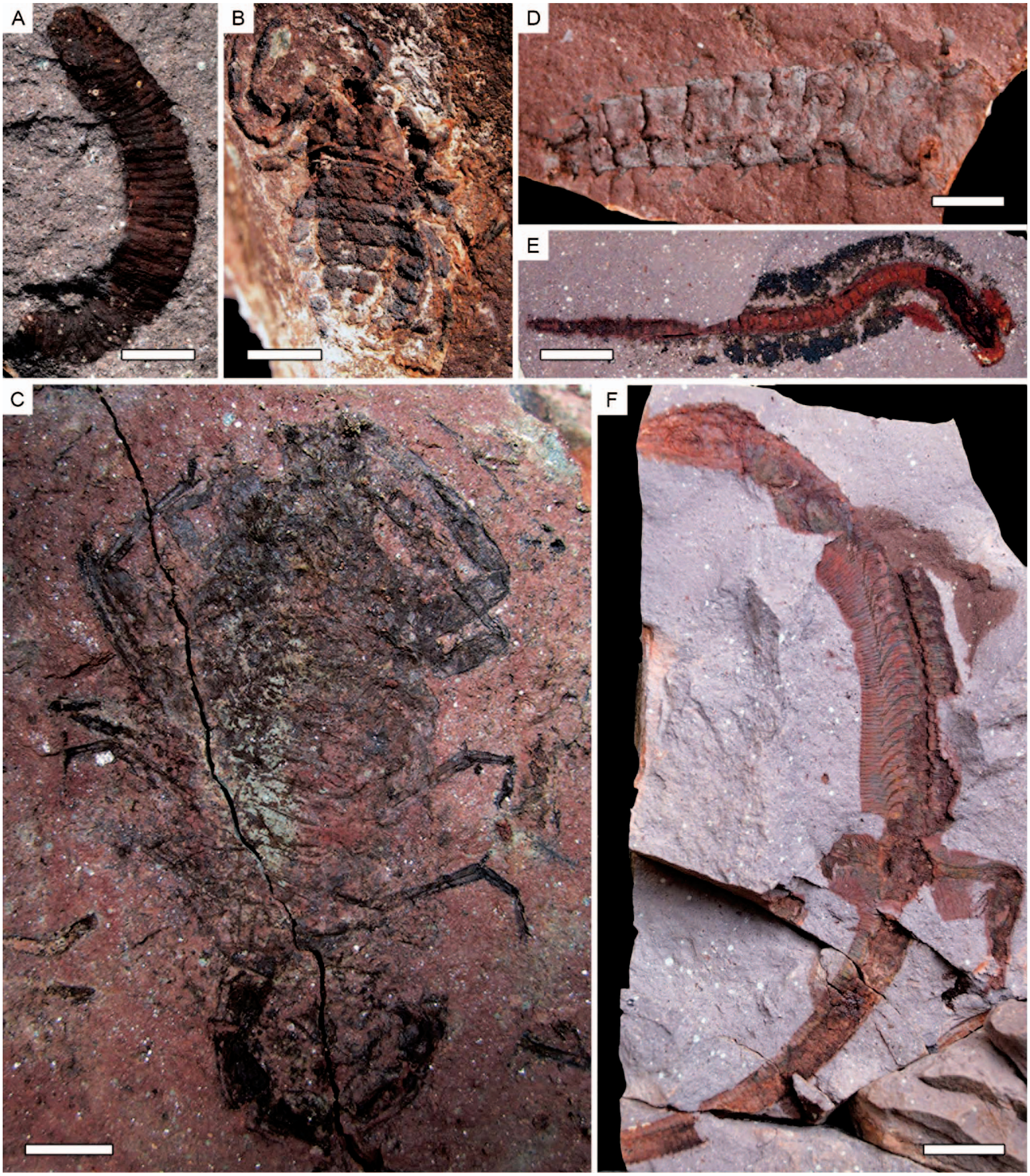

FIGURE 12—Diversity of the animal fossil record. A) Diplopod impression in the tuff of Facies 5.1 (TA0851). Scale bar 7 mm. B) Trigonotarbid arachnid from the tuff of Facies 5.1 (TA0932). Scale bar 3 mm. C) Pulmonate scorpion found in the uppermost paleosol (TA1126). Scale bar 1 cm. D) Leg of the giant millipede *Arthropleura* (TA0884). Scale bar 1 cm. E) Aistopod from the tuff of Facies 5.1 (TA0900). Scale bar 1 cm. F) Complete reptile skeleton from the tuff of Facies 5.1 (TA1045). Scale bar 2 cm.

above stem apices, and upturned strata (Fig. 6A). Although the introduction of VISS as primary structures formed by the interaction of detrital sediments with *in situ* plants was defined for epiclastic environments, we emphasize their application for sequences that originated from the deposition of volcanic ashes and surges. The interaction of volcanic depositional processes with standing vegetation causes phenomena quite similar to that resulting from hydrodynamic and decay-related processes discussed by Rygel et al. (2004). In several units of our section we recognized structures that resulted from transport currents, and supported the interpretation and reconstruction of flow directions and details of entombing processes during eruption events. We can provide examples of further phenomena, such as buildups of plants and pyroclasts in catchment areas (Figs. 10A–B, D) or shadows adjacent to a tree stump formed from eolian currents (Rößler et al., 2009).

Collecting and detailed analysis of the first fallout and flow deposits represented by the different facies of Unit S5, not only provided a rich plant assemblage, but a diverse fauna of vertebrates, arthropods, and gastropods for the first time from this site. These finds will enable a more comprehensive view of this fossil Lagerstätte. In this context, all reptile finds were made in close proximity to large-diameter, upright-standing tree trunks.

Tunger and Eulenberger (1996) came to the conclusion that the specimens hitherto known from the Petrified Forest of Chemnitz are from more than one horizon. Our results confirm this in its entirety. In addition, the first systematic, well-documented excavation will be very helpful for reinterpreting the very rich old museum collections. Typical preservation types can now be assigned to their putative original horizon, and the new material and data also provide information about fossilization processes. On the other hand, lithologic features provide information on diagenetic processes. Compaction effects recognizable from roots, accretionary lapilli, and the upward drag of strata around upright standing trunk bases may enable us to decipher the amount of compaction of the different units and facies and to calculate the primary volume of the pyroclastics. In summary, the forested landscape was destroyed, buried, and fossilized within a very short time and has thus been preserved as a true Permian Pompeii about 290.6 ± 1.8 Ma.

CONCLUSIONS

1. An outstanding lower Permian fossil assemblage has been discovered from the Leukersdorf Formation in the Chemnitz Basin, Germany. Between 2008 and 2011, the first systematic excavation of the Chemnitz Petrified Forest provided more than 1,800 finds of petrifactions and adpressions from different volcaniclastic units and their sedimentary basement.

2. The autochthonous fossil deposit originated from volcanic eruptions and preserved the most complete Permian forest ecosystem known to date.

3. Fifty-three trunk bases, still standing upright in their place of growth and rooting in the underlying paleosol, characterize this fossil Lagerstätte as a significant T^0 assemblage. This window gives insights into a spatially restricted lowland environment that sheltered a dense hygrophilous vegetation of pteridophytes and gymnosperms as well as a diverse fauna of vertebrates, arthropods, and gastropods.

4. The comprehensive dataset of 3D coordinates gathered for every fossil find resulted in a special database and a 3D model applied as research tool to attain fundamental information on the fossilization processes, but also to permit the reconstruction of the ancient vegetation and shed light on their spatial heterogeneity, density, and canopy structure.

5. The fossil record revealed previously unknown biological features, such as organ connections, ontogenetic variability of the branching architecture, and root systems of the occurring arboreal plants.

6. The geological section was documented in depth, and thereby taphonomic phenomena were detected, such as fluid-escape structures, bleaching haloes, catchment areas rich in woody branches, large pyroclasts, and patterns that reveal transport directions.

7. The findings enhance our understanding of plants' responses to environmental perturbations and enable us to visualize and reconstruct individual volcanic events and their effects on the ecosystem.

ACKNOWLEDGMENTS

We thank the many people and companies involved for the financial, material, and personal support making this excavation possible and successful. We gratefully acknowledge both preparation work and scientific discussions of Robert Noll, Tiefenthal; Ralf Werneburg and Georg Sommer, Schleusingen; Christian Ballhaus, Bonn; Christoph Breitkreuz, Silke Sekora, and Ludwig Luthardt, Freiberg; and Dagmar Dietrich, Sven Eulenberger, and Bernd Tunger, Chemnitz. Manfred Barthel, Berlin, kindly contributed to the study and interpretation of the adpression plant fossils, and Bernhard Hausdorf, Hamburg, identified the gastropods. We are indebted to Carole T. Gee, Bonn, Stephen T. Hasiotis, Lawrence, and Lutz Kunzmann, Dresden, for sharing additional information, improving the English usage, and editorial work. Hans Kerp, Münster, and Jean Galtier, Montpellier, provided crucial comments as reviewers of this manuscript. This research was funded in part by the Volkswagen Foundation (Az:I/84638) and the National Natural Science Foundation of China (40902009, 41172006).

REFERENCES

Arakel, A.V., 1986, Evolution of calcrete in paleodrainages of the Lake Napperby area, Central Australia: Palaeogeography, Palaeoclimatology, Palaeoecology, v. 54, p. 283–303.

Barthel, M., 1976, Die Rotliegendflora Sachsens: Abhandlungen des Staatlichen Museums für Mineralogie und Geologie. v. 24, p. 1–190, Dresden.

Barthel, M., 2001, Pflanzengruppen und Vegetationseinheiten der Manebach-Formation: Beiträge zur Geologie von Thüringen, N.F., v. 8, p. 93–123.

Barthel, M., 2003–2008, Die Rotliegendflora des Thüringer Waldes. Teil 1 (2003) Veröffentlichungen Naturhistorisches Museum Schleusingen. v. 18, p. 3–16, Teil 2 (2004). v. 19, p. 19–48, Teil 3 (2005). v. 20, p. 27–56, Teil 4 (2006). v. 21, p. 33–72, Teil 5 (2007). v. 22, p. 41–67, Teil 6 (2008). v. 23, p. 39–62.

Barthel, M., and Rößler, R., 2011, Pflanzen und Pflanzengesellschaften des Rotliegend, *in* Deutsche Stratigraphische Kommission, ed., Stratigraphie von Deutschland X. Rotliegend. Teil 1: Innervariscische Becken: Schriftenreihe der Deutschen Gesellschaft für Geowissenschaften, v. 61, p. 9–27.

Bateman, R.M., 1991, Palaeoecology, *in* Cleal, C.J., ed., Plant Fossils in Geological Investigation: The Palaeozoic: Ellis Horwood Series in Applied Geology, Ellis Horwood Ltd., Chicester, UK, p. 34–116.

Berger, H.-J., and Junghanns, C., 2010, Rotliegend, *in* Alexowsky, W., Berger, H.-J., Hübner, F., Junghanns, C., and Wolf, L., eds., Geologische Karte des Freistaates Sachsen, 1:25,000, Erläuterung zu Blatt 5143 Chemnitz, 4. neu bearbeitete Auflage, Freiberg.

Branney, M.J., and Kokelaar, P., 2002, Pyroclastic density currents and the sedimentation of ignimbrites: Geological Society of London, Memoir, v. 27, p. 1–143.

Cotta, B., 1832, Die Dendrolithen in Bezug auf ihren inneren Bau: Arnoldische Buchhandlung, Leipzig and Dresden, 89 p.

DiMichele, W.A., and Falcon-Lang, H., 2011, Pennsylvanian 'fossil forests' in growth position (T^0 assemblages): Origin, taphonomic bias and palaeoecological insights: Journal of the Geological Society London, v. 168, p. 585–605.

DiMichele, W.A., Kerp, H., and Chaney, D.S., 2004, Tropical floras of the Late Pennsylvanian–early Permian Transition: Carrizo Arroyo in context: New Mexico Museum of Natural History and Sciences Bulletin, v. 25, p. 105–109.

DiMichele, W.A., Tabor, N.J., Chaney, D.S., and Nelson, W.J., 2006, From wetlands to wet spots: Environmental tracking and the fate of Carboniferous elements in early Permian tropical floras: Geological Society of America, Special Paper. v. 399, p. 223–248.

DiMichele, W.A., Cecil, C.B., Chaney, D.S., Elrick, S.D., Lucas, S.G., Lupia, R., Nelson, W.J., and Tabor, N.J., 2011, Pennsylvanian-Permian vegetational changes in tropical Euramerica, *in* Harper, J.A., ed., Geology of the Pennsylvanian-Permian in the Dunkard basin: Guidebook, 76th Annual Field Conference of Pennsylvania Geologists, Washington, Pennsylvania, p. 60–102.

Döring, H., Fischer, F., and Rößler, R., 1999, Sporostratigraphische Korrelation des Rotliegend im Erzgebirge-Becken mit dem Permprofil des Donezk-Beckens: Veröffentlichungen des Museums für Naturkunde Chemnitz, v. 22, p. 29–56.

Druitt, T.H., 1998, Pyroclastic density currents, *in* Gilbert, J.S., and Sparks, R.S.J., eds., The Physics of Explosive Volcanic Eruptions: Geological Society London Special Publication, v. 145, p. 145–182.

Eulenberger, S., Schneider, J.W., and Rößler, R., 2010, Die Kernbohrung KB 6 im basalen Zeisigwald-Tuff von Chemnitz-Hilbersdorf: Veröffentlichungen des Museums für Naturkunde Chemnitz, v. 33, p. 113–122.

Falcon-Lang, H., Jud, N.A., Nelson, J., DiMichele, W.A., Chaney, D.S., and Lucas, S.G., 2011, Pennsylvanian coniferopsid forests in sabkha facies reveal the nature of seasonal tropical biome: Geology, v. 39, p. 371–374.

Feng, Z., Wang, J., and Rößler, R., 2011, A unique gymnosperm from the latest Permian of China, and its ecophysiological implications: Review of Palaeobotany and Palynology, v. 165, p. 27–40.

Fischer, F., 1990, Lithologie und Genese des Zeisigwald-Tuffs (Rotliegendes, Vorerzgebirgs-Senke): Veröffentlichungen des Museums für Naturkunde Chemnitz, v. 14, p. 61–74.

Galtier, J., 2008, A new look at the permineralized flora of Grand-Croix (Late Pennsylvanian, Saint-Etienne basin, France): Review of Palaeobotany and Palynology, v. 152, p. 129–140.

Galtier, J., Ronchi, A., and Broutin, J., 2011, Early Permian silicified floras from the Perdasdefogu Basin (SE Sardinia): Comparison and bio-chronostratigraphic correlation with the floras of the Autun Basin (Massif central, France): Geodiversitas, v. 33, p. 43–69.

Hilton, J., Wang, S.J., Galtier, J., and Li, C.S., 2001, An early Permian plant assemblage from the Taiyuan Formation of northern China with compression/impression and permineralized preservation: Review of Palaeobotany and Palynology, v. 114, p. 175–189.

Hilton, J., Wang, S.J., Galtier, J., Glasspool, I., and Stevens, L., 2004, An upper Permian permineralized plant assemblage in volcaniclastic tuff from the Xuanwei Formation, Guizhou Province, southern China, and its palaeofloristic significance: Geological Magazine, v. 141, p. 661–674.

Hinz, J.K., Smith, I., Pfretzschner, H.-U., Wings, O., and Sun, G., 2010, A high-resolution three-dimensional reconstruction of a fossil forest (Upper Jurassic Shishugou Formation, Junggar Basin, Northwest China): Palaeobiodiversity and Palaeoenvironments, v. 90, p. 215–240.

Jenik, J., 1978, Roots and root systems in tropical trees: Morphologic and ecologic aspects, *in* Tomlinson, P.B., and Zimmermann, M.H., eds., Tropical Trees as Living Systems: Cambridge University Press, Cambridge, UK, p. 323–349.

Kerp, H., 1996, Post-Variscian late Palaeozoic Northern Hemisphere gymnosperms: The onset to the Mesozoic: Review of Palaeobotany and Palynology, v. 90, p. 263–285.

Kerp, J.H.F., Poort, R.J., Swinkels, H.A.J.M., and Verwer, R., 1990, Aspects of Permian palaeobotany and palynology, IX. Conifer-dominated Rotliegend Floras from the Saar-Nahe-Basin (?Late Carboniferous–early Permian; SW-Germany) with special reference to the reproductive biology of early conifers: Review of Palaeobotany and Palynology, v. 62, p. 205–248.

Kretzschmar, R., Annacker, V., Eulenberger, S., Tunger, B., and Rößler, R., 2008, Erste wissenschaftliche Grabung im Versteinerten Wald von Chemnitz: Ein Zwischenbericht: Freiberger Forschungsheft, v. C 528, p. 25–55.

Krings, M., Taylor, T.N., Dotzler, N., and Galtier, J., 2011, Fungal remains in cordaite (Cordaitales) leaves from the Upper Pennsylvanian of central France: Bulletin of Geosciences, v. 86, p. 777–784.

Libertín, M., Opluštil, S., Pšenička, J., Bek, J., Sýkorová, I., and Dašková, J., 2009, Middle Pennsylvanian pioneer plant assemblage buried in situ by volcanic ash-fall, central Bohemia: Czech Republic Review of Palaeobotany and Palynology, v. 155, p. 104–133.

Montañez, I.P., Tabor, N.J., Niemeier, D., DiMichele, W.A., Frank, T.D., Fielding, C.R., Isbell, J.L., Birgenheier, L.P., and Rygel, M.C., 2007, CO_2-forced climate and vegetation instability during late Paleozoic deglaciation: Science, v. 315, p. 87–91.

Nestler, K., Dietrich, D., Witke, K., Rößler, R., and Marx, G., 2003, Thermogravimetric and RAMAN Spectroscopic Investigations on Different Coals in Comparison to Dispersed Anthracite Found in Permineralized Tree Fern *Psaronius* sp.: Journal of Molecular Structure, v. 661–662, p. 357–362.

Opluštil, S., Pšenička, J., Libertín, M., and Šimůnek, Z., 2007, Vegetation patterns of Westphalian and Lower Stephanian mire assemblages preserved in tuff beds of the continental basins of Czech Republic: Review of Palaeobotany and Palynology, v. 143, p. 107–154.

Opluštil, S., Pšenička, J., Libertín, M., Bashforth, A.R., Šimůnek, Z., Drábková, J., and Dašková, J., 2009, A Middle Pennsylvanian (Bolsovian) peat-forming forest preserved in situ in volcanic ash of the Whetstone Horizon in the Radnice Basin, Czech Republic: Review of Palaeobotany and Palynology, v. 155, p. 234–274.

Pfefferkorn, H.W., and Wang, J., 2009, *Stigmariopsis, Stigmaria asiatica*, and the survival of the *Sigillaria brardii-ichthyolepis* group in the tropics of the late Pennsylvanian and early Permian: Palaeoworld, v. 18, p. 130–135.

Retallack, G.J., 2001, Soils of the Past, 2nd edition: Blackwell, Oxford and Northhampton, UK, 404 p.

Rex, G.M., 1986, The preservation and palaeoecology of the Lower Carboniferous silicified plant deposits at Esnost, near Autun, France: Geobios, v. 19, p. 773–800.

Roscher, M., and Schneider, J.W., 2006, Permo-Carboniferous climate: Early Pennsylvanian to late Permian climate development of central Europe in a regional and global context, *in* Lucas, S.G., Cassinis, G., and Schneider, J.W., eds., Non-Marine Permian Biostratigraphy and Biochronology: Geological Society London Special Publication, v. 265, p. 95–136.

Rößler, R., 2000, The late Palaeozoic tree fern *Psaronius*: An ecosystem unto itself: Review of Palaeobotany and Palynology, v. 108, p. 55–74.

Rößler, R., ed., 2001, Der Versteinerte Wald von Chemnitz: Katalog zur Ausstellung Sterzeleanum, Museum für Naturkunde, Chemnitz, Germany, 253 p.

Rößler, R., 2006, Two remarkable Permian petrified forests: Correlation, comparison and significance, *in* Lucas, S.G., Cassinis, G., and Schneider, J.W., eds., Non-Marine Permian Biostratigraphy and Biochronology: Geological Society London Special Publication, v. 265, p. 39–63.

Rößler, R., and Barthel, M., 1998, Rotliegend taphocoenoses preservation favoured by rhyolithic explosive volcanism: Freiberger Forschungsheft, v. C 474, p. 59–101.

Rößler, R., and Noll, R., 2006, Sphenopsids of the Permian (I): The largest known anatomically preserved calamite, an exceptional find from the petrified forest of Chemnitz, Germany: Review of Palaeobotany and Palynology, v. 140, p. 145–162.

Rößler, R., and Noll, R., 2007, *Calamitea* Cotta, the correct name for calamitean sphenopsids currently classified as *Calamodendron* Brongniart: Review of Palaeobotany and Palynology, v. 144, p.157–180.

Rößler, R., and Noll, R., 2010, Anatomy and branching of *Arthropitys bistriata* (Cotta) Goeppert: New observations from the Permian petrified forest of Chemnitz, Germany: International Journal of Coal Geology, v. 83, p. 103–124.

Rößler, R., Kretzschmar, R., Annacker, V., and Mehlhorn, S., 2009, Auf Schatzsuche in Chemnitz: Wissenschaftliche Grabungen ’09: Veröffentlichungen des Museums für Naturkunde Chemnitz, v. 32, p. 25–46.

Rößler, R., Kretzschmar, R., Annacker, V., Mehlhorn, S., Merbitz, M., Schneider, J.W., and Luthardt, L., 2010, Auf Schatzsuche in Chemnitz: Wissenschaftliche Grabungen ’10: Veröffentlichungen des Museums für Naturkunde Chemnitz, v. 33, p. 27–50.

Rößler, R., Feng, Z., and Noll, R. 2012, The largest calamite and its growth architecture: *Arthropitys bistriata* from the Permian petrified forest of Chemnitz: Review of Palaeobotany and Palynology, v. 185, p. 64–78.

Rygel, M.C., Gibling, M.R. and Calder, J.H., 2004, Vegetation-induced sedimentary structures from fossil forests in the Pennsylvanian Joggins Formation, Nova Scotia: Sedimentology, v. 51, p. 531–552.

Schneider, J.W., and Werneburg, R., 2011, Biostratigraphie des Rotliegend mit Insekten und Amphibien, *in* Deutsche Stratigraphische Kommission, ed., Stratigraphie von Deutschland X. Rotliegend. Teil I: Innervariscische Becken: Schriftenreihe der Deutschen Gesellschaft für Geowissenschaften, v. 61, p. 110–142.

Schneider, J.W., Rößler, R., and Gaitzsch, B., 1995, Time lines of the late Variscan volcanism: Holostratigraphic synthesis: Zentralblatt Geologie Paläontologie, Teil I, v. 5/6, p. 477–490.

Schneider, J.W., Lucas, S.G., Werneburg, R., and Rößler, R., 2010, Euramerican Late Pennsylvanian/early Permian arthropleurid/tetrapod associations: Implications for the habitat and paleobiology of the largest terrestrial arthropod, *in* Lucas, S.G., Schneider, J.W., and Spielmann, J., 2010, eds., Carboniferous–Permian Transition in Canon del Cobre, Northern New Mexico: New Mexico Museum of Natural History and Science Bulletin, v. 49, p. 49–70.

Schneider, J.W., Rößler, R., and Fischer, F., 2011, Rotliegend des Chemnitz-Beckens, *in* Deutsche Stratigraphische Kommission, ed., Stratigraphie von Deutschland X. Rotliegend. Teil I: Innervariscische Becken: Schriftenreihe der Deutschen Gesellschaft für Geowissenschaften, v. 61, p. 319–377.

Schumacher, R., and Schmincke, H.-U., 1991, Internal structure and occurrence of accretionary lapilli: A case study at Laacher See volcano: Bulletin of Volcanology, v. 53, p. 612–634.

Shute, C.H., and Cleal, C.J., 1987, Palaeobotany in museums: Geological Curator, v. 4, no. 9, p. 553–559.

Sterzel, J.T., 1875, Die fossilen Pflanzen des Rothliegenden von Chemnitz in der Geschichte der Palaeontologie: Berichte der Naturwissenschaftlichen Gesellschaft Chemnitz, v. 5, p. 71–243.

Sterzel, J.T., 1918, Die organischen Reste des Kulms und des Rotliegenden der Gegend von Chemnitz: Abhandlungen der Königlich Sächsischen Gesellschaft der Wissenschaften, Mathematisch-physikalische Klasse, B.G. Teubner Verlagsgesellschaft, Leipzig, v. 35, no. 5, p. 205–315,

Taylor, T.N., Taylor, E.L., and Krings, M., 2009, Paleobotany, the Biology and Evolution of Fossil Plants, 2nd edition: Academic Press, Elsevier, 1230 p.

Trewin, N.H., 1994, Depositional environment and preservation of biota in the Lower Devonian hot-springs of Rhynie, Aberdeenshire, Scotland: Transactions of the Royal Society of Edinburgh: Earth Sciences, v. 84, p. 433–442.

Tunger, B., and Eulenberger, S., 1996, Versteinertes Holz von Chemnitz: Neufunde von 1990 bis 1995: Veröffentlichungen des Museums für Naturkunde Chemnitz, v. 19, p. 35–48.

Wagner, R.H., 1989, A late Stephanian forest swamp with Sporangiostrobus fossilized by volcanic ash fall in the Puertollano Basin, central Spain: International Journal of Coal Geology, v. 12, p. 523–552.

Weber, O., and Sterzel, J.T., 1896, Beiträge zur Kenntnis der Medulloseae: Berichte der Naturwissenschaftlichen Gesellschaft Chemnitz, v. 13, p. 44–143.

Werneburg, R., and Schneider, J.W., 2006, Amphibian biostratigraphy of the European Permo-Carboniferous, *in* Lucas, S.G., Cassinis, G., and Schneider, J.W., eds., Non-Marine Permian Biostratigraphy and Biochronology: Geological Society London Special Publication, v. 265, p. 201–215.

ACCEPTED JUNE 16, 2012